This article has been accepted for publication in a future issue of this journal, but has not been fully edited. Content may change prior to final publication. Citation information: DOI 10.1109/TWC.2017.2713777, IEEE Transactions on Wireless Communications



# Time-Domain Turbo Equalization for Single-Carrier Generalized Spatial Modulation

Lixia Xiao, Yue Xiao, *Member, IEEE*, Yan Zhao, *Member, IEEE*, Ping Yang, *Senior member, IEEE*, Marco Di Renzo, *Senior member, IEEE*, Shaoqian Li, *Fellow, IEEE*, and Wei Xiang, *Senior member, IEEE*

***Abstract*—In this paper, low-complexity time-domain turbo equalization (TDTE) detectors based upon the soft-interference-cancellation (SIC)-aided minimum mean-square error (MMSE) criterion are proposed for single carrier (SC) generalized spatial modulation (GSM) (SC-GSM) systems. First, a symbol-by-symbol (SS)-aided TDTE (SS-TDTE) detector for application to the small-scale GSM systems is proposed, where the zero symbols are considered as constellation points when performing SIC. Then, vector-by-vector (VV)-aided TDTE (VV-TDTE) detectors for application to larger-scale antenna systems are introduced, where the GSM symbol is treated as an entire vector when performing SIC. As for the proposed VV-TDTE detectors, in addition, different time-varying filter coefficients are designed, in order to strike a flexible trade-off between complexity and performance. By relying upon extrinsic information transfer (EXIT) chart analysis, we show that the proposed TDTE detectors are capable of providing considerable bit error rate (BER) performance gains over existing TDTE detectors and over the classic frequency-domain equalization (FDE) based MMSE detector, especially for the unbalanced antenna configurations.**

***Index Terms*—Spatial modulation (SM), generalized spatial modulation (GSM), turbo equalization, minimum mean-square error (MMSE)**

## I. Introduction

GENERALIZED spatial modulation (GSM) [1]-[3], which is the extension of spatial modulation [4]-[9], is a novel low-complexity energy-efficient multiple-input multiple-output (MIMO) transmission technique. In GSM, more than one but not all the transmit antennas are activated to convey different information symbols. As a result, GSM is capable of striking a flexible trade-off between SM and spatial multiplexing (e. g. V-BLAST [10]). GSM is also able to improve the energy-efficiency, since fewer radio-frequency chains than conventional MIMO systems [10] [11] are needed. In general, several independent studies have proved that SM and GSM are promising candidates for large-scale antenna MIMO designs [12]-[13].

Recently, the issues of transceiver design, spatial constellation optimization, link adaptation, distributed/cooperative protocols and iterative detection with various forward error correction codes were investigated in [14]-[22]. Despite the rich literature [1]-[22], SM-based designs have been predominantly investigated in the context of flat fading channels, which would tacitly imply that orthogonal frequency division multiplexing needs to be employed for application to wide-band frequency-selective channels [23] [24]. In this case, multiple radio-frequency chains have to be used, which will negate most of the benefits of GSM. To circumvent this problem, the family of single-carrier (SC) transmission [25], which can retain the benefits of GSM, has become an interesting and promising alternative for application to broadband GSM.

As far as SC-GSM is concerned, there are three options for adding the prefix to eliminate the inter block interference (IBI), i) the non-prefix option [26], ii) the cyclic prefix (CP) option [27]-[30] and iii) the zero prefix (ZP) option [31]-[34]. Specially, it has been demonstrated in [31]-[34] that ZP-aided SC-GSM (ZP-SC-GSM) is capable of obtaining full multipath diversity and a better bit error rate (BER) performance than its CP-aided and non-prefix-aided counterparts. In this paper, as a consequence, our research efforts are focused on ZP-SC-GSM system. For ZP-SC-GSM system, classical frequency-domain equalization (FDE) detectors [30] do not constitute effective means to mitigate the IBI encountered in dispersive channel since the ZP prefix cannot turn the linear convolution into a circular convolution. Time domain equalization (TDE), on the other hand, is a better choice for application to ZP-SC-GSM. Recently, various low-complexity hard-decision TDE algorithms have been proposed for the uncoded ZP-SC-GSM system [33] [34], which are aimed to approach maximum-likelihood (ML) detection performance at a reduced complexity. These solutions, however, may be not directly applicable to the coded ZP-SC-GSM systems, which require soft-input soft-output detectors to fully realize the expected coding gains.

Time-domain turbo equalization (TDTE) [35] [36] is an effective iterative detection scheme for eliminating the IBI of the coded conventional MIMO system over dispersive channels, which relies on the iterative exchange of soft information, in the form of log-likelihood ratios

L. Xiao, Y. Xiao, Y. Zhao, P. Yang, and S. Li are with the National Key Laboratory of Science and Technology on Communications, University of Electronic Science and Technology of China 611731, Sichuan, China.

Y. Xiao is also with Science and Technology on Electronic Information Control Laboratory, the 29th Research Institute of China Electronics Technology Group Corporation.

The corresponding author is Y. Xiao (xiaoyue@uestc.edu.cn).

Marco Di Renzo is with the Laboratory of Laboratoire des Signaux et Systèmes, CNRS, CentraleSupélec, Univ Paris Sud, Université Paris-Saclay, 3 rue Joliot Curie, Plateau du Moulon, 91192, Gif-sur-Yvette, France. (e-mail: marco.direnzo@l2s.centralesupelec.fr).

W. Xiang is with the College of Science, Technology and Engineering, James Cook University, Cairns, QLD 4878, Australia (e-mail: wei.xiang@jcu.edu.au).

The financial support is gratefully acknowledged by the National Science Foundation of China under Grant numbers 61501095 and 61671131, the Fundamental Research Funds for the Central Universities (No. ZYGX2015J011), the Foundation Project of Science and Technology on Electronic Information Control Laboratory under Grant JS17041403811 and ZTE Industry-Academia-Research Cooperation Funds.

This article has been accepted for publication in a future issue of this journal, but has not been fully edited. Content may change prior to final publication. Citation information: DOI 10.1109/TWC.2017.2713777, IEEE Transactions on Wireless Communications



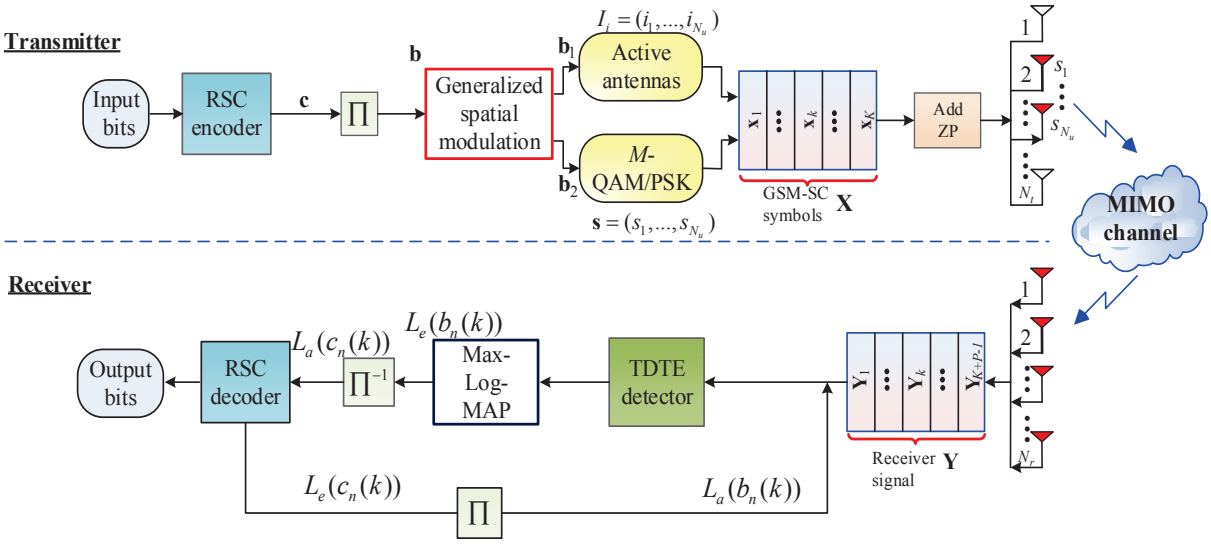


Fig. 1. System model of the coded ZP-SC-GSM system with the TDTE receiver.

(LLRs), between the equalizer and the decoder. Several low-complexity TDTE detectors for conventional space-time MIMO schemes exist in the literature [37] [38]. In these implementations, the LLRs of the encoded bits of each symbol emitted by the TAs can be computed at the output of the soft interference cancellation (SIC) and minimum mean-square error (MMSE) detector. These approaches, however, cannot be directly applied to ZP-SC-GSM. The reason lies in the fact that GSM symbol includes the zero symbol in the constellation diagram, which does not allow the LLRs to be calculated directly. To the best of the authors' knowledge, the design of soft-decision (SoD)-aided iterative detector for the coded ZP-SC-GSM system has not yet been investigated. Against the above background, the major contributions of this paper are summarized as follows.

1) The performances of the coded ZP-SC-GSM system under both perfect and imperfect channel estimation are firstly studied and compared. Specifically, the existing hard-decision detectors of the ZP-SC-GSM system are extended to their SoD versions and their limitations are introduced. To address these limitations, an improved symbol-by-symbol (SS) TDTE (SS-TDTE) detector [38] is proposed for the coded ZP-SC-GSM system based on the special transmit structure of GSM symbols, which is capable of achieving a near-capacity performance and has not been investigated before;
2) Furthermore, in order to reduce the complexity of the proposed SS-TDTE detector, two effective vector-by-vector (VV) TDTE detectors are proposed for the coded ZP-SC-GSM system, where the GSM symbol in each time slot is treated as a vector in the SIC stage. Also, various MMSE filter coefficients are designed to provide a good trade-off in terms of complexity and performance;
3) We employ the extrinsic information transfer (EXIT) chart analysis [40] to study the convergence of the proposed TDTE detectors. The maximum achievable limits of the proposed TDTE detectors for balanced and unbalanced antenna configurations are investigated using the EXIT chart. Moreover, simulation results are presented to demonstrate that the ZP-SC-GSM system based upon the proposed TDTE detectors are capable of providing considerable BER performance gains over the ZP-SC-V-BLAST system based on the TDTE detector in [38] and the CP-SC-GSM system based on the classical FDE-based MMSE detector of [30].

The remainder of this paper is organized as follows. Section II gives a brief review of ZP-SC-GSM and of its conventional hard-decision detectors. Also, we propose the corresponding SoD detectors. In Section III, we propose a novel TDTE detector based on the SS-aided MMSE principle. In Section IV, two VV-aided TDTE detectors are proposed for a large-scale antennas system. In Section V, the iterative convergence and maximum achievable limits of the proposed detectors are analyzed using EXIT chart analysis. The BER performance is presented in Section VI. Finally, Section VII concludes this paper.

Notation: $(\cdot)^{-1}$, $(\cdot)^T$ and $(\cdot)^H$ represent the pseudo inverse, transpose and Hermitian transpose operators, respectively. $\mathbf{0}_{m\times n}$ denotes the $(m \times n)$-dimensional null matrix with all zeros. $\mathbf{1}_{m\times n}$ represents the $(m \times n)$-dimensional matrix with all ones. $\mathbf{I}_m$ is the $(m \times m)$ identity matrix. $\|\cdot\|_2$ denotes the 2-norm of a matrix. $|\cdot|$ indicates the cardinality of a given set or the amplitude of a complex number. $\mathsf{diag}(\cdot)$ refers to the operation of reshaping a vector to a diagonal matrix. $\bar{x}$ is the mean value of $x$.

## II. ZP-SC-GSM System Model and Conventional TDTE Detection

We consider a GSM-MIMO system with $N_t$ transmit and $N_r$ receive antennas over a dispersive channel, which has $P$ multi-path links between each antenna pair. The system model of the coded ZP-SC-GSM system with iterative TDTE detection is illustrated in Fig. 1. As can be seen from Fig. 1, the source information bits are channel encoded by a recursive systematic convolutional (RSC) code. Then, these encoded bits $\mathbf{c}$ are interleaved with the aid of a random bit interleaver $\Pi$. The interleaved bit stream is divided into vectors of $KB$ bits each, where $K$ is the number of GSM symbols in one frame, and $B$ is the

This article has been accepted for publication in a future issue of this journal, but has not been fully edited. Content may change prior to final publication. Citation information: DOI 10.1109/TWC.2017.2713777, IEEE Transactions on Wireless Communications



number of bits that each GSM symbol carries. Subsequently, each vector $\mathbf{b}=[b_1,...,b_{KB}]$ is split into $K$ sub-vectors $\mathbf{b}(k)=[b_1(k),...,b_B(k)]$, $k=(1,...,K)$ with a length of $B$ bits and then mapped to a GSM symbol $\mathbf{x}_k$. After GSM mapping, the corresponding transmit block of the $K$ GSM-mapped symbols is formed as $[\mathbf{x}_1,...,\mathbf{x}_k,...,\mathbf{x}_K]\in\mathbb{C}^{N_t\times K}$, and the $(P-1)$ zeros are added to each data frame before transmission. Moreover, we usually have $K\gg(P-1)$ to get the high data transmission rate. At the receiver, iterative detection is implemented through exchanging the extrinsic information in the form of LLRs between the channel decoder and the TDTE detector. Specifically, the receive signal consisting of $K'=K+P-1$ time instants can be written as

$$\underbrace{\begin{bmatrix}\mathbf{y}_1\\ \mathbf{y}_2\\ \vdots\\ \mathbf{y}_{K'}\end{bmatrix}}_{\mathbf{y}}=\underbrace{\begin{bmatrix}\mathbf{H}_0 & \cdots & \mathbf{O}\\ \vdots & \cdots & \vdots\\ \mathbf{H}_{P-1} & \ddots & \mathbf{O}\\ \mathbf{O} & \cdots & \mathbf{H}_0\\ \vdots & \ddots & \vdots\\ \mathbf{O} & \cdots & \mathbf{H}_{P-1}\end{bmatrix}}_{\mathbf{H}\text{ of size }N_rK'\times N_tK}\underbrace{\begin{bmatrix}\mathbf{x}_1\\ \mathbf{x}_2\\ \vdots\\ \mathbf{x}_K\end{bmatrix}}_{\mathbf{x}}+\underbrace{\begin{bmatrix}\mathbf{n}_1\\ \mathbf{n}_2\\ \vdots\\ \mathbf{n}_{K'}\end{bmatrix}}_{\mathbf{n}}, \tag{1}$$

where $\mathbf{x}_k\in\mathbb{C}^{N_t\times 1}$ and $\mathbf{y}_k\in\mathbb{C}^{N_r\times 1}$ denote transmit and receiver vectors in the $k$-th time slot, respectively, and $\mathbf{x}=[(\mathbf{x}_1)^T,...,(\mathbf{x}_K)^T]^T$ is a row vector of size $KN_t\times 1$. Moreover, $\mathbf{H}_j\in\mathbb{C}^{N_r\times N_t}$ is the channel matrix of the $j$-th path, and $\mathbf{n}_k\in\mathbb{C}^{N_r\times 1}$ denotes the noise vector. The elements of channel matrices and noise vector are assumed to follow the complex Gaussian distribution $\mathcal{CN}(0,1/P)$ and $\mathcal{CN}\left(0,\sigma_0^2\right)$, respectively.

In GSM, $N_u$ out of $N_t$ ($N_u<N_t$) transmit antennas are activated to transmit the information bit vector $\mathbf{b}$. Only $T=2^{\lfloor\log_2(C_{N_t}^{N_u})\rfloor}$ transmit antenna combinations (TACs) are permitted for modulating the information bits, where $C_{N_t}^{N_u}$ denotes the binomial coefficient and $\lfloor\cdot\rfloor$ is the floor operator. In each time slot, the information bit vector $\mathbf{b}$ of length $B$ bits is divided into two parts: 1) $B_1=\log_2(T)$ bits are assigned to select one TAC $I_i=(i_1,...,i_{N_u})$ and 2) $B_2=N_u\log_2(L)$ bits are assigned to modulate $N_u$ $L$-PSK symbols that are transmitted by the active TAC. So, the resultant $k$-th GSM transmit vector can be expressed as

$$\mathbf{x}_k=[...,0,s_1,0,...,0,s_2,0...,0,s_{N_u},0,...]^T. \tag{2}$$

### A. Optimal Detection

As shown in [35], the optimal detector of estimating the uncoded bit $\hat{c}_g\in\{0,1\}$ can be obtained by maximizing the *a posteriori* probability (APP) $P(\hat{c}_g=a|\mathbf{y})$ as

$$\hat{c}_g=\arg\max_{a\in\{0,1\}}P(c_g=a|\mathbf{y}). \tag{3}$$

An algorithm that achieves the above objective is commonly referred to as a maximum *a posteriori* probability (MAP) algorithm, which is expressed as

$$P(c_g=a|\mathbf{y})=\sum_{\forall\mathbf{c}:c_g=a}P(a|\mathbf{y})=\sum_{\forall\mathbf{c}:c_g=a}\frac{P(\mathbf{y}|\mathbf{c})P(\mathbf{c})}{P(\mathbf{y})}. \tag{4}$$

where the probability $P(\mathbf{c})=\prod_{i=1}^{Q}P(c_i)$ is the *a priori* probability of the sequence $\mathbf{c}=[c_1,...,c_Q]$. According to (4), the conditional LLR $L(c_g|\mathbf{y})$ are given by

$$L(c_g|\mathbf{y})=\ln\frac{\sum_{\forall\mathbf{c}:c_g=1}P(\mathbf{y}|\mathbf{c})\prod_{i=1,i\neq g}^{Q}P(c_i)}{\sum_{\forall\mathbf{c}:c_g=0}P(\mathbf{y}|\mathbf{c})\prod_{i=1,i\neq g}^{Q}P(c_i)}+L_a(c_g). \tag{5}$$

where $L_a(c_g)$ is the *a prior* probability. However, as stated in [35] that the MAP algorithm for optimal joint equalization and decoding is usually impractical, a standard approach to reducing the computational burden of the receiver is to split the detection problem into two subproblems, i.e., equalization and decoding. Next, we will introduce two distinct families of algorithms for the subproblem of equalization including ML sequence detection and MAP symbol detection (MAP-SD).

**ML-aided TDTE Detector:** The ML sequence detector computes an estimate $\hat{\mathbf{x}}$ of the entire sequence $\mathbf{x}$ by maximizing the likelihood $p(\mathbf{y}|\mathbf{x})$. The LLRs $L(b_m|\mathbf{y})$ $(m=1,...,KB)$ of the encoded bits $\mathbf{b}=[b_1,...,b_{KB}]$ that the entire sequence $\mathbf{x}$ carried can be expressed as

$$L(b_m|\mathbf{y})=\underbrace{\ln\frac{\sum_{\forall\mathbf{x}:b_m=1}P(\mathbf{y}|\mathbf{x})\prod_{i=1,i\neq m}^{KB}P(b_i)}{\sum_{\forall\mathbf{x}:b_m=0}P(\mathbf{y}|\mathbf{x})\prod_{i=1,i\neq m}^{KB}P(b_i)}}_{L_e(b_m)}+L_a(b_m), \tag{6}$$

where the extrinsic information LLRs $L_e(b_m)$ $(m=1,...KB)$ can be written using the Max-Log rule [22] as

$$L_e(b_m)=\max_{\mathbf{x}\in\chi_1^m}(d_m)-\max_{\mathbf{x}\in\chi_0^m}(d_m),(m=1,...,KB), \tag{7}$$

where $\chi_1^m$ and $\chi_0^m$ represent the subset of set $\chi$ that satisfy $\chi_1^m=\{\mathbf{x}\in\chi\text{: }b_m=1\}$ and $\chi_0^m=\{\mathbf{x}\in\chi\text{: }b_m=0\}$, respectively and we have the probability metric $d_m$ as [22]

$$d_m=-\frac{\|\mathbf{Y}-\mathbf{H}\mathbf{x}\|_2^2}{\sigma_0^2}+\sum_{j=1,j\neq m}^{KB}b_jL_a(b_j), \tag{8}$$

where $b_j$ denotes the $j$-th encoded bit of $\mathbf{b}$ and $L_a(b_j)$ is the *a priori* LLR produced by the channel decoder.

**MAP-SD-aided TDTE Detector:** The MAP-SD-aided TDTE detector yields an estimate $\hat{\mathbf{x}}_k$ by maximizing the likelihood $p(\mathbf{y}|\mathbf{x}_k)$. The conditional LLRs $L(b_n(k)|\mathbf{y})$, $n=1,...,B$ $k=1,...,K$ of encoded bits $\mathbf{b}(k)=[b_1(k),...,b_B(k)]$ that $\hat{\mathbf{x}}_k$ carries can be expressed as

$$L(b_n(k)|\mathbf{y})=\underbrace{\ln\frac{\sum_{\forall\mathbf{x}_k:b_n(k)=1}P(\mathbf{y}|\mathbf{x}_k)\prod_{i=1,i\neq n}^{B}P(b_i(k))}{\sum_{\forall\mathbf{x}_k:b_n(k)=0}P(\mathbf{y}|\mathbf{x}_k)\prod_{i=1,i\neq n}^{B}P(b_i(k))}}_{L_e(b_n(k))}+L_a(b_n(k)). \tag{9}$$

In MAP-SD, the effect of the ISI channel can be regarded as a different form of error protection, i.e., a rate-1 convolutional code. The conditional LLRs $L(b_n(k)|\mathbf{y})$ can be further obtained by the classic Bahl-Cocke-Jelinek-

Raviv (BCJR) algorithm [35]

$$L(b_n(k)|\mathbf{y}) = \ln \frac{\sum\limits_{\forall s,s' \in \mathcal{S}: b_n(k)=1} \alpha_k(s)\gamma_k(s,s')\beta_{k+1}(s)}{\sum\limits_{\forall s,s' \in \mathcal{S}: b_n(k)=0} \alpha_k(s)\gamma_k(s,s')\beta_{k+1}(s)}, \tag{10}$$

where $\mathcal{S}$ is the set of channel states of cardinality $2^{B(P-1)}$, $\alpha_k(s)$ is the probability of the channel state $s$ in the $k$-th time slot computed by the probabilities of channel states in the $(k-1)$-th time slot, $\beta_{k+1}(s)$ is the probability of the channel state $s$ in the $k$-th time slot computed by the possible probabilities of the channel states in the $(k+1)$-th time slot, and $\gamma_k(s,s')$ is the transformational probability from state $s$ to state $s'$ in the $k$-th time slot, which can be computed as in [35].

Additionally, based on the signal model given in (1), there exist only two low-complexity TDE-aided hard-decision algorithms for ZP-SC-GSM systems: i) the partial interference cancellation receiver with successive interference cancellation (PIC-R-SIC) detector [31] and ii) the tree search aided $M$-algorithm detector [34]. Next, their SoD-aided counterparts are developed.

### B. Existing Hard-Decision Extension

**PIC-R-SIC-Aided TDTE Detector:** The PIC-R-SIC-aided TDTE detector computes an estimate $\hat{\mathbf{x}}_k$ by maximizing the likelihood $p(\mathbf{y}|\mathbf{x}_k)$. The extrinsic information LLRs $(L_e(b_n(K)), ..., L_e(b_n(k)), ..., L_e(b_n(1))$ $(n = 1, ..., B))$ of the $k$-th GSM symbol $\mathbf{x}_k$, in particular, can be summarized as follows.

**Step 1:** Construct a new receiver signal $\mathbf{z}_{I_k}$ [31]. Firstly, remove the interference imposed by the GSM symbols $\mathbf{x}_{k+1}, \mathbf{x}_{k+2}, ..., \mathbf{x}_K$, which can be obtained $\mathbf{y}^{(k)} = \sum\limits_{i=1}^{k} \mathbf{G}_{I_i}\mathbf{x}_i + \mathbf{n}$. Then, a projection matrix $\mathbf{P}_{I_k} = \mathbf{I}_{N_r K'} - \mathbf{Q}_{I_k}$ is multiplied by $\mathbf{y}^{(k)}$, where $\mathbf{Q}_{I_k} = \mathbf{G}^c_{I_k}((\mathbf{G}^c_{I_k})^H \mathbf{G}^c_{I_k})^{-1}(\mathbf{G}^c_{I_k})^H$ and $\mathbf{G}^c_{I_k} = [\mathbf{G}_{I_1}, \mathbf{G}_{I_2}, ..., \mathbf{G}_{I_{k-1}}]$ . After multiplying $\mathbf{P}_{I_k}$ by $\mathbf{y}^{(k)}$, we have $\mathbf{z}_{I_k} = \mathbf{P}_{I_k}\mathbf{y}^{(k)}$.

**Step 2:** Compute the probability metric $d_n^k$ as follows

$$d_n^k = -\frac{\|\mathbf{z}_{I_k} - \mathbf{P}_{I_k}\mathbf{G}_{I_k}\mathbf{x}_k\|_2^2}{\sigma_0^2} + \sum_{u=1, u\neq n}^{B} b_u(k) L_a(b_u(k)). \tag{11}$$

**Step 3:** Calculate the LLRs $L_e(b_n(k))$ by using the Max-Log rule as

$$L_e(b_n(k)) = \max_{\mathbf{x}_k \in \mathbb{S}_1^n}(d_n^k) - \max_{\mathbf{x}_k \in \mathbb{S}_0^n}(d_n^k), (n = 1, ..., B), \tag{12}$$

where $\mathbb{S}_1^n$ and $\mathbb{S}_0^n$ represent the subset of the GSM symbol set $\mathbb{S}$, which satisfy $\mathbb{S}_1^n = \{\mathbf{x}_k \in \mathbb{S}: b_n(k) = 1\}$ and $\mathbb{S}_0^n = \{\mathbf{x}_k \in \mathbb{S}: b_n(k) = 0\}$, respectively.

**M-Algorithm-Aided TDTE Detector:** The M-Algorithm-Aided TDTE Detector computes an estimate $\hat{\mathbf{x}}$ of the reduced sequence $\mathbf{x}$ set by maximizing the likelihood $p(\mathbf{y}|\mathbf{x})$. Denoting by $\phi$ the set of the $M$ candidate vectors, the LLRs $L_e(b_m)$ can be written based on (6)-(7) as

$$L_e(b_m) = \max_{\mathbf{x} \in \phi_1^m}(d_m) - \max_{\mathbf{x} \in \phi_0^m}(d_m), (m = 1, ..., KB), \tag{13}$$

where $\phi_1^m$ and $\phi_0^m$ represent the subset of set $\phi$, that satisfy $\phi_1^m = \{\mathbf{x} \in \phi: b_m = 1\}$ and $\phi_0^m = \{\mathbf{x} \in \phi: b_m = 0\}$, respectively. If set $\phi_1^m$ or set $\phi_0^m$ is null, detection can be performed by using the algorithm in [22].

### C. Limitation of Conventional TDTE Detectors

Firstly, for the ML-aided TDTE detector, the size of the search space is reaching $2^{BK}$. The complexity of the decoder will be intractable and the implementation of the detector will be impractical for large values of $B$ and $K$.

For the MAP-SD-aided TDTE detector, the size of the channel states is reaching $2^{B(P-1)}$, which result in high complexity for large values of $B$ and $P$.

For the PIC-R-SIC-aided TDTE detector, it is demonstrated in [34] that the PIC-R-SIC detector is only suitable if $(K + P - 1)N_r \geq (K - 1)N_t$. Additionally, the construction of the new receiver signal $\mathbf{z}_{I_k}$ requires large-dimensional MMSE or zero forcing operations, which may impose high complexity for large value of $K$.

For the $M$-algorithm-aided TDTE detector, the LLRs obtained only by $M$ candidates, which may suffer from some performance loss compared with its PIC-R-SIC-aided and ML-aided counterparts.

Among the TDTE detectors for the conventional space-time MIMO system, the MMSE-aided TDTE detector in [38] is a promising alternative, which can achieve a near-capacity performance with low-complexity. However, for the ZP-SC-GSM system, each GSM symbol includes zero symbols and the index of the TAC also conveys information. So the MMSE-aided TDTE detector in [38] is not directly applicable to the coded ZP-SC-GSM system. In the next section, the MMSE-aided TDTE detector of [38] and its limitation will be introduced in detail.

## III. Proposed Symbol-by-Symbol-Aided TDTE Detector

### A. Conventional TDTE Detector [38]

In this section, we give a brief review of conventional TDTE [38] detector and introduce the limitations for its application to ZP-SC-GSM. In [38], the TDTE detector is designed for the V-BLAST system. When transmit symbol vector $\mathbf{x}_k$ $(k = 1, ..., K)$ of (1) are the V-BLAST symbols, the TDTE detector of [38] can be performed, where the vector $\mathbf{x}_k$ is the $k$-th V-BLAST symbol as

$$\mathbf{x}_k = [x_k^1, x_k^2, ..., x_k^{N_t}]^T, \tag{14}$$

where $x_k^q$ $q = (1, ..., N_t)$ is the $L$-PSK symbol carrying $l = \log_2(L)$ bits as $\mathbf{b}_q(k) = [b_{(q-1)l+1}(k), ..., b_{ql}(k)]$. In [38], the extrinsic LLRs $L_e(b_n(k))$ of $\mathbf{b}_q(k)$ corresponding to $x_k^q$ is computed based on MMSE-aided detector as follows

$$L_e(b_n(k)) = \ln \frac{P(b_n(k) = 1|\mathbf{y}(k))}{P(b_n(k) = 0|\mathbf{y}(k))}, n = ((q-1)l+1, ..., ql), \tag{15}$$

where $\mathbf{y}(k)$ is the received signal of $N = N_1 + N_2 + 1$ time slots in (1), which can be expressed as

$$\mathbf{y}(k) = [\mathbf{y}_{k-N_2}^T, ..., \mathbf{y}_k^T, \mathbf{y}_{k+1}^T, ..., \mathbf{y}_{k+N_1}^T]^T = \hat{\mathbf{H}}\mathbf{s}(k) + \mathbf{n}(k), \tag{16}$$

where we have $\mathbf{s}(k) = [\mathbf{x}_{k-P-N_2+1}^T, ..., \mathbf{x}_k^T, \mathbf{x}_{k+1}^T, ..., \mathbf{x}_{k+N_1}^T]^T$, $\mathbf{n}(k) = [\mathbf{n}_{k-P-N_2+1}^T, ..., \mathbf{n}_{k+N_1}^T]^T$ and $\hat{\mathbf{H}}$ is the sub-channel matrix of size $NN_r \times (N+P-1)N_t$ given by

$$\hat{\mathbf{H}} = \begin{bmatrix} \mathbf{H}_{P-1} & \cdots & \mathbf{H}_0 & \cdots & \mathbf{O} \\ \vdots & \ddots & \vdots & \ldots & \vdots \\ \mathbf{O} & \cdots & \mathbf{H}_{P-1} & \cdots & \mathbf{H}_0 \end{bmatrix}. \tag{17}$$

This article has been accepted for publication in a future issue of this journal, but has not been fully edited. Content may change prior to final publication. Citation information: DOI 10.1109/TWC.2017.2713777, IEEE Transactions on Wireless Communications



On the other hand, the LLRs produced by the channel decoder are taken as the *priori* LLRs $L_a(b_n(k))$ of $\mathbf{b}_q(k)$, which can be expressed as

$$L_a(b_n(k))=\ln\frac{P(b_n(k)=1)}{P(b_n(k)=0)}, n=((q-1)l+1,...,ql), \quad (18)$$

where $P(b_n(k)=1)$ and $P(b_n(k)=0)$ denote the probability of $b_n(k)=1$ and $b_n(k)=0$, respectively, which can be computed as

$$P(b_n(k)=0)=\frac{1}{1+e^{L_a(b_n(k))}}, P(b_n(k)=1)=\frac{e^{L_a(b_n(k))}}{1+e^{L_a(b_n(k))}}. \quad (19)$$

Moreover, the values of $L_e(b_n(k))$ is obtained by the *priori* LLRs $L_a(b_n(k))$, which is introduced as follows.

**Step 1**: Compute the mean and variance of the transmit signal $x_k^q$ as

$$\bar{x}_k^q \triangleq E(x_k^q)=\sum_{\alpha\in\mathbb{A}}\alpha P(x_k^q=\alpha), \quad (20)$$

$$v_k^q \triangleq (\sum_{\alpha\in\mathbb{A}}|\alpha|^2 P(x_k^q=\alpha))-|\bar{x}_k^q|^2, \quad (21)$$

where $\mathbb{A}$ is the set of $L$-PSK symbols, and $P(x_k^q=\alpha)$ is the probability of $x_k^q=\alpha$. Assuming that the constellation point $\alpha$ is mapped by the binary bits $\mathbf{b}_\alpha=[b_1,...b_l]$, the value of $P(x_k^q=\alpha)$ is obtained as

$$P(x_k^q=\alpha)=\prod_{i=1}^{l}P(b_{(q-1)+i}(k)=b_i), \quad (22)$$

where $b_i\in[0,1]$. Consequently, one can calculate the mean $\bar{\mathbf{x}}_k=[\bar{x}_k^1,\bar{x}_k^2,...,\bar{x}_k^{N_t}]^T$ and variance $\mathbf{v}_k=[v_k^1,v_k^2,...,v_k^{N_t}]^T$ of $\mathbf{x}_k$ using (14)-(17). Then the mean and variance of the transmit vector $\mathbf{s}(k)$ in (11) can be expressed as

$$\begin{aligned}\bar{\mathbf{s}}(k)&=[\bar{\mathbf{x}}_{k-P+1}^T,...,\bar{\mathbf{x}}_k^T,\bar{\mathbf{x}}_{k+1}^T,...,\bar{\mathbf{x}}_{k+P-1}^T]^T\\ \mathbf{v}(k)&=[\mathbf{v}_{k-P+1}^T,...,\mathbf{v}_k^T,\mathbf{v}_{k+1}^T,...,\mathbf{v}_{k+P-1}^T]^T.\end{aligned} \quad (23)$$

**Step 2**: Apply SIC to the $q$-th symbol in the $k$-th time slot. The receiver signal after SIC is given as $\mathbf{r}(k)=\mathbf{y}(k)-\hat{\mathbf{H}}\hat{\mathbf{s}}(k)$, where $\hat{\mathbf{s}}(k)=[\bar{\mathbf{x}}_{k-P+1}^T,...,\hat{\mathbf{x}}_k^T,\bar{\mathbf{x}}_{k+1}^T,...,\bar{\mathbf{x}}_{k+P-1}^T]^T$ with $\hat{\mathbf{x}}_k=[\bar{x}_k^1,...,\bar{x}_k^{q-1},0,\bar{x}_k^{q+1},...,\bar{x}_{N_t}]^T$.

**Step 3**: Perform MMSE detection. The $q$-th symbol of $\mathbf{x}_k$ can be estimated as $\hat{x}_k^q=(\mathbf{c}_k^q)^H\mathbf{r}(k)$ using the MMSE criterion, where $\mathbf{c}_k^q=(\hat{\mathbf{H}}\hat{\mathbf{V}}(k^q)\hat{\mathbf{H}}^H+\sigma_0^2\mathbf{I}_{NN_r})^{-1}\mathbf{h}_s$ and $s=(P+N_2-1)N_t+q$, where $\mathbf{h}_s$ is the $s$-th column of $\hat{\mathbf{H}}$. We have

$$\hat{\mathbf{V}}(k^q)=\mathsf{diag}[\mathbf{v}_{k-P+1}^T,...,\hat{\mathbf{v}}_k^T,\mathbf{v}_{k+1}^T,...,\mathbf{v}_{k+P-1}^T], \quad (24)$$

where $\hat{\mathbf{v}}(k)=[v_k^1,...,v_k^{q-1},1,v_k^{q+1},...,v_k^{N_t}]$.

**Step 4**: Calculate the LLRs based on the estimated $\hat{x}_k^q$. The estimated $\hat{x}_k^q$ can be assumed to follow a Gaussian distribution of $\mathcal{CN}(u_k,\sigma_k)$, and an approximate conditional probability density function (CPDF) of the estimated $\hat{x}_k^q$ is give by

$$P(\hat{x}_k^q=\alpha|\hat{\mathbf{H}})\propto\exp(-|\hat{x}_k^q-u_k|^2/\sigma_k^2), \quad (25)$$

where $u_k$ and $\sigma_k^2$ can be obtained as

$$u_k=(\mathbf{c}_k^q)^H\mathbf{h}_s\alpha, \sigma_k^2=(\mathbf{c}_k^q)^H\mathbf{h}_s-(\mathbf{c}_k^q)^H\mathbf{h}_s\mathbf{h}_s^H\mathbf{c}_k^q, \quad (26)$$

where $\alpha$ is one of constellation symbols in set $\mathbb{A}$. As a result, it follows from the Max-Log rule that the LLRs of $b_n(k)$ is given by

$$\begin{aligned}L_e(b_n(k))=&\max_{\alpha\in\mathbb{A}_1^n}\frac{-|\hat{x}_k^q-u_k|^2}{\sigma_k^2}+\sum_{u\neq n}(b_u(k))L_a(b_u(k))\\ &-\max_{\alpha\in\mathbb{A}_0^n}\frac{-|\hat{x}_k^q-u_k|^2}{\sigma_k^2}+\sum_{u\neq n}(b_u(k))L_a(b_u(k)),\end{aligned} \quad (27)$$

where $\mathbb{A}_0^n$ and $\mathbb{A}_1^n$ represent two subsets of set $\mathbb{A}$ that satisfy $\mathbb{A}_0^n=\{\alpha\in\mathbb{A}: b_n(k)=0\}$ and $\mathbb{A}_1^n=\{\alpha\in\mathbb{A}: b_n(k)=1\}$.

If a V-BLAST scheme is considered, step 1 and step 4 can be performed directly, since the $N_t$ symbols of the $N_t$ TAs are independent and each symbol $x_k^q$ carries $l$ encoded bits. If ZP-SC-GSM is considered, on the other hand, the transmitted $N_t$ symbols $x_k^q$ $(q=1,...,N_t)$ have zero symbols and are not independent of each other, since they are the basic modulation unit in GSM-based systems. Moreover, the number of bits carried by the the symbol $x_k^q$ becomes uncertain, so that the *priori* LLRs corresponding to the symbol $x_k^q$ cannot be obtained by (27) directly. Based on these observations, it is found that the terms of $\bar{x}_k^q$ in the vector $\bar{\mathbf{x}}_k$ and the terms of $v_k^q$ in the vector $\mathbf{v}_k$ cannot be computed symbol-by-symbol, meanwhile it is also challenge to obtain the extrinsic LLRs corresponding to the symbol $x_k^q$. As a result, the conventional TDTE detector conceived for VBLAST in [38] is not suitable for the coded ZP-SC-GSM system.

### *B. Proposed SS-TDTE*

In this section, a novel SS-aided TDTE detector for application to ZP-SC-GSM is proposed. In the proposed SS-TDTE detector, the zero symbol is viewed as a constellation point in the SIC process and MMSE decoding. At each time slot, the LLRs of the encoded bits of one GSM symbol are jointly calculated from the $N_t$ symbols of the $N_t$ TAs, instead of from the symbols of each TA separately.

Similar to the conventional TDTE detector [38], the soft output of the MMSE-aided turbo equalizer is obtained by utilizing the received signal of $(N=N_1+N_2+1)$ time slots in (1). Thus, the detection can be performed based on (16), where $\mathbf{x}_k$ is a GSM symbol. There are two main differences between the conventional TDTE detector and the proposed SS-TDTE detector: 1) the mean and variance of the signal vector $\mathbf{s}(k)$ in (16) are computed by relying on a vector-by-vector basis instead of a symbol-by-symbol basis and 2) the extrinsic information LLRs of the encoded bits at the $k$-th time slot are calculated based on a vector-by-vector basis. The iterative process of the proposed SS-TDTE is detailed below.

**Step 1**: Obtain the mean and variance of the transmit signal $\mathbf{s}(k)$ in (16) based on the *priori* LLRs $L_a(b_n(k))$. In ZP-SC-GSM, $N_t$ symbols of the $N_t$ TAs are not independent and constitute a GSM symbol vector. To compute the mean and variance, as a result, the GSM symbol is considered as a whole, as follows

$$\bar{\mathbf{x}}_k \triangleq E(\mathbf{x}_k)=\sum_{\boldsymbol{\beta}\in\mathbb{S}}\boldsymbol{\beta}\cdot P(\mathbf{x}_k=\boldsymbol{\beta}), \quad (28)$$

$$\mathbf{v}_k \triangleq (\sum_{\boldsymbol{\beta}\in\mathbb{S}}|\boldsymbol{\beta}|^2\cdot P(\mathbf{x}_k=\boldsymbol{\beta}))-|\bar{\mathbf{x}}_k|^2, \quad (29)$$

where $P(\mathbf{x}_k = \boldsymbol{\beta})$ is the probability of $\mathbf{x}_k = \boldsymbol{\beta}$, which can be expressed as

$$P(\mathbf{x}_k = \boldsymbol{\beta}) = \prod_{n=1}^{B} \frac{e^{(b_n(k))L_a(b_n(k))}}{1 + e^{L_a(b_n(k))}}. \tag{30}$$

Then, the mean and variance of the $k$-th GSM symbol vector $\mathbf{x}_k$ can be formulated as

$$\begin{aligned} \bar{\mathbf{x}}_k &= [\bar{x}_k^1, ..., \bar{x}_k^{q-1}, \bar{x}_k^q, \bar{x}_k^{q+1}, ..., \bar{x}_k^{N_t}]^T, \\ \mathbf{v}_k &= [v_k^1, ..., v_k^{q-1}, v_k^q, v_k^{q+1}, ..., v_k^{N_t}]^T, \end{aligned} \tag{31}$$

where $q = (1, ..., N_t)$. Finally, the mean and variance vector of the transmit signal $\mathbf{s}(k)$ in (16) can be obtained based on (28)-(31) as

$$\begin{aligned} \bar{\mathbf{s}}(k) &= [\bar{\mathbf{x}}_{k-P-N_2+1}^T, ..., \bar{\mathbf{x}}_k^T, \bar{\mathbf{x}}_{k+1}^T, ..., \bar{\mathbf{x}}_{k+N_1}^T]^T \\ \mathbf{v}(k) &= [\mathbf{v}_{k-P-N_2+1}^T, ..., \mathbf{v}_k^T, \mathbf{v}_{k+1}^T, ..., \mathbf{v}_{k+N_1}^T]^T. \end{aligned} \tag{32}$$

In the proposed SS-TDTE detector, in particular, we first compute the mean and variance of the entire GSM vector and then obtain the mean and variance of each symbol transmitted by a TA. This is different from the conventional TDTE detector.

**Step 2**: Apply SIC to the $q$-th symbol in the $k$-th time slot. In this step, the zero symbol of the GSM constellation is considered as a zero point, and the mean and variance of this symbol can be obtained via (31). Thus, SIC can be carried out similar to the conventional TDTE detector [38] in a symbol-by-symbol manner.

**Step 3**: Perform MMSE detection. Similar to the conventional TDTE detector.

**Step 4**: Calculate the LLRs based on the estimated $\hat{x}_k^q$. Since the zero symbol is treated as a constellation point, the estimated $\hat{x}_k^q$ can also be assumed to follow a Gaussian distribution of $\mathcal{CN}(u_{k,s}, \sigma_{k,s})$, and an approximate CPDF of the estimated $\hat{x}_k^q$ is as follows

$$P(\hat{x}_k^q = \hat{\alpha} | \hat{\mathbf{H}}) \propto \exp(-|\hat{x}_k^q - u_{k,s}|^2 / \sigma_{k,s}^2). \tag{33}$$

where $u_{k,s}$ and $\sigma_{k,s}^2$ can be obtained as

$$\begin{aligned} u_{k,s} &= (\mathbf{c}_k^q)^H \mathbf{h}_s \hat{\alpha}, \\ \sigma_{k,s}^2 &= (\mathbf{c}_k^q)^H \mathbf{h}_s - (\mathbf{c}_k^q)^H \mathbf{h}_s \mathbf{h}_s^H \mathbf{c}_k^q, \end{aligned} \tag{34}$$

where $\hat{\alpha}$ is one of symbols in set $\hat{\mathbb{A}} = [\mathbb{A}, 0]$.

In ZP-SC-GSM, as mentioned above, the number of encoded bits that the estimated symbol $\hat{x}_k^q$ carries is uncertain, so that the corresponding extrinsic information LLRs cannot be directly calculated by the CPDF in (25). In the proposed SS-TDTE detector, to solve this issue, the extrinsic information LLRs corresponding to the estimated $\hat{x}_k^q$ are obtained by jointly utilizing the $N_t$ estimated probabilities of $P(\hat{x}_k^q = \hat{\alpha} | \hat{\mathbf{H}})(q = 1, ..., N_t)$. The $N_t$ estimated symbols $\hat{\mathbf{x}}_k = [\hat{x}_k^1, ..., \hat{x}_k^q, ..., \hat{x}_k^{N_t}]$ may correspond to one GSM symbol vector with $\boldsymbol{\beta}_i = [\beta_i^1, ...\beta_i^q, ..., \beta_i^{N_t}]$ $(i = 1, ..., 2^B)$, where $\boldsymbol{\beta}_i \in \mathbb{S}$ and $\beta_i^q \in \hat{\mathbb{A}}$. The probability of $\hat{\mathbf{x}}_k = \boldsymbol{\beta}_i$ is given by

$$P(\hat{\mathbf{x}}_k = \boldsymbol{\beta}_i) = \prod_{q=1}^{N_t} P(\hat{x}_k^q = \beta_i^q | \hat{\mathbf{H}}). \tag{35}$$

As a result, according to (33)-(35), the extrinsic information LLRs $L_e(b_n(k))$ $(n = 1, ..., B)$, $(k = 1, ..., K)$ corresponding to the transmitted symbol $\mathbf{x}_k$ are given by

$$L_e(b_n(k)) = \max_{\boldsymbol{\beta}_i \in \mathbb{S}_1^n} (P(\hat{\mathbf{x}}_k = \boldsymbol{\beta}_i)) - \max_{\boldsymbol{\beta}_i \in \mathbb{S}_0^n} (P(\hat{\mathbf{x}}_k = \boldsymbol{\beta}_i)). \tag{36}$$

## IV. Proposed Vector-by-Vector-Aided TDTE Detectors

In the proposed SS-TDTE detector in (36), the calculation of the LLRs $L_e(b_n(k))(n = 1, .., B)$ requires the knowledge of the probability $P(\hat{\mathbf{x}}_k = \boldsymbol{\beta}_i)$ in (35) and the calculation of $\mathbf{c}_k^q$ needs to be computed by $N_t$ times, which may impose high complexity for high rate transmission systems. To circumvent this problem, two novel VV-TDTE detectors are proposed in this section, for application to ZP-SC-GSM systems. In the proposed detectors, the GSM symbol is always treated as a vector in the SIC process. To avoid the calculations of (35) and $\mathbf{c}_k^q$, however, the entire GSM vector of $N_t$ symbols is estimated. This is possible thanks to the design of novel MMSE filter coefficients. In particular, different MMSE filter coefficients are designed for application to the proposed VV-TDTE detectors in order to strike a flexible trade-off between performance and complexity. Similar to the proposed SS-TDTE detector, the calculation of the LLRs, in the proposed VV-TDTE detectors, are based on the system model in (11), where $\mathbf{x}_k$ is substituted by a GSM symbol.

### A. Proposed VV-TDTE Detector

In the proposed VV-TDTE detectors, the MMSE filter coefficients are different from those in [38], which are designed based on the SS principle. In this section, thus, we first introduce the details of the MMSE filter design. Based on the MMSE principle, the estimated transmit vector $\hat{\mathbf{x}}_k \in \mathbb{C}^{N_t \times 1}$ corresponding to the observed signal $\mathbf{y}(k)$ can be written as follows

$$\hat{\mathbf{x}}_k = \mathbf{C}_k^H \mathbf{y}(k) + \mathbf{b}_k, \tag{37}$$

where $\mathbf{C}_k \in \mathbb{C}^{NN_r \times N_t}$ and $\mathbf{b}_k \in \mathbb{C}^{N_t \times 1}$ are the coefficients of the MMSE estimator. From the MMSE estimation principle, we have

$$(\mathbf{C}_k, \mathbf{b}_k) = \underset{\substack{\mathbf{C}_k \in \mathbb{C}^{NN_r \times N_t} \\ \mathbf{b}_k \in \mathbb{C}^{N_t \times 1}}}{\arg\min} (E\{\|\mathbf{x}_k - \hat{\mathbf{x}}_k\|_2^2\}). \tag{38}$$

The solutions of (38) need to satisfy the following conditions

$$\begin{aligned} \frac{\partial E\{\|\mathbf{x}_k - \hat{\mathbf{x}}_k\|_2^2\}}{\partial \mathbf{C}_k^H} &= -2 \cdot E\{(\mathbf{x}_k - \hat{\mathbf{x}}_k)\mathbf{y}(k)^H\} = \mathbf{0}_{N_t \times NN_r} \\ \frac{\partial E\{\|\mathbf{x}_k - \hat{\mathbf{x}}_k\|_2^2\}}{\partial \mathbf{b}_k} &= -2 \cdot E\{(\mathbf{x}_k - \hat{\mathbf{x}}_k)\} = \mathbf{0}_{N_t \times 1}. \end{aligned} \tag{39}$$

By substituting (16) and (39) in (37), the MMSE-based linear filter coefficients $\mathbf{C}_k$ and $\mathbf{b}_k$ are obtained as

$$\begin{aligned} \mathbf{C}_k &= \mathbf{Cov}(\mathbf{y}(k), \mathbf{y}(k))^{-1} \mathbf{Cov}(\mathbf{y}(k), \mathbf{x}_k) \\ \mathbf{b}_k &= \bar{\mathbf{x}}_k - \mathbf{C}_k^H E(\mathbf{y}(k)), \end{aligned} \tag{40}$$

where $\mathbf{Cov}(s, t) = E(st^H) - E(s)E(t^H)$. Substituting (40) in (37), the estimated transmit vector $\hat{\mathbf{x}}_k$ is as follows

$$\hat{\mathbf{x}}_k = \bar{\mathbf{x}}_k + \mathbf{Cov}(\mathbf{x}_k, \mathbf{y}(k))(\mathbf{y}(k), \mathbf{y}(k))^{-1}(\mathbf{y}(k) - E(\mathbf{y}(k))). \tag{41}$$

This article has been accepted for publication in a future issue of this journal, but has not been fully edited. Content may change prior to final publication. Citation information: DOI 10.1109/TWC.2017.2713777, IEEE Transactions on Wireless Communications



Based on the received signal model in (16), $E(\mathbf{y}(k))$, $\mathbf{Cov}(\mathbf{x}_k, \mathbf{y}(k))$ and $\mathbf{Cov}(\mathbf{y}(k), \mathbf{y}(k))$ in (41) can be estimated as follows

$$\begin{aligned} &E(\mathbf{y}(k)) = \hat{\mathbf{H}}\bar{\mathbf{s}}(k) \\ &\mathbf{Cov}(\mathbf{x}_k, \mathbf{y}(k)) = \mathbf{Cov}(\mathbf{x}_k, \mathbf{x}_k)[\mathbf{0}_{N_t \times N_2^{'}} \mathbf{1}_{N_t \times 1} \mathbf{0}_{N_t \times N_1}]\hat{\mathbf{H}}^H \\ &\mathbf{Cov}(\mathbf{y}(k), \mathbf{y}(k)) = \sigma_0^2 \mathbf{I}_{(NN_r)} + \hat{\mathbf{H}}\mathrm{Cov}(\mathbf{s}(k), \mathbf{s}(k))\hat{\mathbf{H}}^H, \end{aligned} \tag{42}$$

where $N_2^{'} = (N_2 + P - 1)$. By substituting (42) in (41), $\hat{\mathbf{x}}_k$ can be estimated as follows

$$\begin{aligned} \hat{\mathbf{x}}_k = \bar{\mathbf{x}}_k + \mathbf{V}_k^d \hat{\mathbf{H}}_{\mathbf{s}}^H (\sigma_0^2 \mathbf{I}_{(NN_r)} + \hat{\mathbf{H}}\mathbf{V}(k)\hat{\mathbf{H}}^H)^{-1} \\ \times (\mathbf{y}(k) - \hat{\mathbf{H}}\bar{\mathbf{s}}(k)), \end{aligned} \tag{43}$$

where we have

$$\begin{aligned} &\bar{\mathbf{s}}(k) = [\bar{\mathbf{x}}_{k-P-N_2+1}^T, ..., \bar{\mathbf{x}}_k^T, ..., \bar{\mathbf{x}}_{k+N_1}^T]^T \\ &\mathbf{V}_k^d = \mathsf{diag}[\mathbf{v}_k] \\ &\mathbf{V}(k) = \mathsf{diag}[\mathbf{v}_{k-P-N_2+1}^T, ..., \mathbf{v}_k^T, ..., \mathbf{v}_{k+N_1}^T] \\ &\hat{\mathbf{H}}_{\mathbf{s}} = \hat{\mathbf{H}}[\mathbf{0}_{N_t \times (N_2+P-1)}, \mathbf{1}_{N_t \times 1}, \mathbf{0}_{N_t \times N_1}]^T, \end{aligned} \tag{44}$$

and $\bar{\mathbf{x}}_t (t \in (k-P-N_2+1, k+N_1))$ and $\mathbf{v}_t \in \mathbb{C}^{N_t \times 1}$ represent the mean and variance vector of the transmit signal $\mathbf{x}_t$, respectively. From (43), we note that the estimated $\hat{\mathbf{x}}_k$ depends on $\bar{\mathbf{x}}_k$, $\mathbf{v}_k$, $\bar{\mathbf{s}}(k)$ and $\mathbf{V}(k)$, which can be obtained by the *priori* LLRs that are fed back from the channel decoder. In order to ensure that $\hat{\mathbf{x}}_k$ is independent of the LLRs of the encoded bits of $\mathbf{x}_k$, we set $\{L(b_n(k))\}_{n=1}^B = \mathbf{0}_{B \times 1}$ when computing $\hat{\mathbf{x}}_k$, which yields $\bar{\mathbf{x}}_k = \mathbf{0}_{N_t \times 1}$, and $\mathbf{V}_k^d = \mathbf{I}_{N_t}$. Hence, the final estimate of $\hat{\mathbf{x}}_k$ can be simplified to

$$\begin{aligned} \hat{\mathbf{x}}_k &= \hat{\mathbf{H}}_{\mathbf{s}}^H (\sigma_0^2 \mathbf{I}_{(NN_r)} + \hat{\mathbf{H}}\hat{\mathbf{V}}(k)\hat{\mathbf{H}}^H)^{-1} (\mathbf{y}(k) - \hat{\mathbf{H}}\hat{\mathbf{s}}(k)) \\ &= \mathbf{C}_k^H (\mathbf{y}(k) - \hat{\mathbf{H}}\hat{\mathbf{s}}(k)) \end{aligned}, \tag{45}$$

where

$$\begin{aligned} &\hat{\mathbf{s}}(k) = [\bar{\mathbf{x}}_{k-P-N_2+1}^T, ..., \bar{\mathbf{x}}_{k-1}^T, \mathbf{0}_{N_t \times 1}^T, \bar{\mathbf{x}}_{k+1}^T, ..., \bar{\mathbf{x}}_{k+N_1}^T]^T \\ &\hat{\mathbf{V}}(k) = \mathsf{diag}[\mathbf{v}_{k-P-N_2+1}^T, ..., \mathbf{v}_{k-1}^T, \mathbf{1}_{N_t \times 1}^T, \mathbf{v}_{k+1}^T, ..., \mathbf{v}_{k+N_1}^T] \\ &\mathbf{C}_k = (\sigma_0^2 \mathbf{I}_{(NN_r)} + \hat{\mathbf{H}}\hat{\mathbf{V}}(k)\hat{\mathbf{H}}^H)^{-1} \hat{\mathbf{H}}_{\mathbf{s}}. \end{aligned} \tag{46}$$

As shown in (45) and (46), the mean and variance of the transmit GSM symbols play an important role in estimating $\hat{\mathbf{x}}_k$. Based on (45) and (46), in particular, the proposed VV-TDTE detector still consists of four steps as follows.

**Step 1**: Obtain the mean vector $\hat{\mathbf{s}}(k)$ and the variance vector $\hat{\mathbf{V}}(k)$ in (45) using (28) and (29), respectively.

**Step 2**: Apply SIC to the $k$-th GSM symbol. In this step, the GSM symbol is treated as a vector as a whole to perform SIC. According to (45), the received signal after SIC is expressed as

$$\mathbf{r}(k) = \mathbf{y}(k) - \hat{\mathbf{H}}\hat{\mathbf{s}}(k). \tag{47}$$

**Step 3**: Perform MMSE detection. Based (45), after performing VV-aided SIC, the estimated signal $\hat{\mathbf{x}}_k$ can be obtained by multiplying the MMSE filter coefficient as

$$\hat{\mathbf{x}}_k = \mathbf{C}_k^H \mathbf{r}(k), \tag{48}$$

where $\mathbf{C}_k$ follows from (46).

**step 4**: Calculate the extrinsic information LLRs. Based on (48), $\hat{\mathbf{x}}_k$ is the estimated vector. Since, in the proposed SS-TDTE detector, it is a vector and not a symbol, the LLR cannot be directly calculated based on the conventional CPDF in (25) and (33). Moreover, the purpose of the proposed VV-TDTE detector is to approximate the CPDF of the estimated signal $\hat{\mathbf{x}}_k$. Assuming that each element $\hat{x}_k^q$ of $\hat{\mathbf{x}}_k$ follows a complex Gaussian distribution, then the term $\exp(-\|\hat{\mathbf{x}}_k - \mathbf{u}_k\|_2^2/\sigma_{k,v}^2)$ follows a chi-square distribution with $2N_t$ degrees, where $\mathbf{u}_k$ and $\sigma_{k,v}^2$ denote the mean and variance of $\hat{\mathbf{x}}_k$, respectively. Accordingly, the CPDF of the estimated vector $\hat{\mathbf{x}}_k$ can be approximated as

$$P(\hat{\mathbf{x}}_k = \boldsymbol{\beta}_i | \hat{\mathbf{H}}) \propto \exp(-\|\hat{\mathbf{x}}_k - \mathbf{u}_k\|_2^2/\sigma_{k,v}^2), \tag{49}$$

where $\boldsymbol{\beta}_i \in \mathbb{S}$. Based on (48), $\mathbf{u}_k$ can be obtained as follows

$$\begin{aligned} \mathbf{u}_k &= E(\hat{\mathbf{x}}_k \,|\mathbf{x}_k = \boldsymbol{\beta}_i\,) \\ &= \mathbf{C}_k^H E(\mathbf{y}(k) - \hat{\mathbf{H}}\hat{\mathbf{s}}(k)\,|\mathbf{x}_k = \boldsymbol{\beta}_i\,) \\ &= \mathbf{C}_k^H \hat{\mathbf{H}}_{\mathbf{s}} \boldsymbol{\beta}_i. \end{aligned} \tag{50}$$

and $\sigma_{k,v}^2$ is equal to

$$\sigma_{k,v}^2 = \|\mathbf{Cov}(\hat{\mathbf{x}}_k, \hat{\mathbf{x}}_k | \mathbf{x}_k = \boldsymbol{\beta}_i)\|_2, \tag{51}$$

where

$$\begin{aligned} &\mathbf{Cov}(\hat{\mathbf{x}}_k, \hat{\mathbf{x}}_k | \mathbf{x}_k = \boldsymbol{\beta}_i) \\ &= \mathbf{C}_k^H \mathrm{Cov}(\mathbf{y}(k) - \hat{\mathbf{H}}\hat{\mathbf{s}}(k), \mathbf{y}(k) - \hat{\mathbf{H}}\hat{\mathbf{s}}(k)\,|\mathbf{x}_k = \boldsymbol{\beta}_i\,)\mathbf{C}_k \\ &= \mathbf{C}_k^H (\mathrm{Cov}(\mathbf{y}(k), \mathbf{y}(k) | \mathbf{x}_k = \boldsymbol{\beta}_i)\mathbf{C}_k \\ &= \mathbf{C}_k^H (\sigma^2 \mathbf{I}_{(NN_r)} + \hat{\mathbf{H}}\mathbf{V}(k)\hat{\mathbf{H}}^H - \hat{\mathbf{H}}_{\mathbf{s}} \mathbf{V}_k^d \hat{\mathbf{H}}_{\mathbf{s}}^H)\mathbf{C}_k \\ &= \mathbf{C}_k^H \hat{\mathbf{H}}_{\mathbf{s}} - \mathbf{C}_k^H \hat{\mathbf{H}}_{\mathbf{s}} \hat{\mathbf{H}}_{\mathbf{s}}^H \mathbf{C}_k | \mathbf{V}_k^d = \mathbf{I}_{N_t}. \end{aligned} \tag{52}$$

From (49), the output extrinsic information $L_e(b_n(k))(n = 1, ..., B, k = 1, ..., K)$ of the proposed VV-TDTE detector is given as

$$L_e(b_n(k)) = \ln \frac{\sum\limits_{\boldsymbol{\beta}_i \in \mathbb{S}_1^n} P(\hat{\mathbf{x}}_k = \boldsymbol{\beta}_i | \hat{\mathbf{H}}) \prod\limits_{u \neq n} e^{(b_u(k)) L_a(b_u(k))}}{\sum\limits_{\boldsymbol{\beta}_i \in \mathbb{S}_0^n} P(\hat{\mathbf{x}}_k = \boldsymbol{\beta}_i | \hat{\mathbf{H}}) \prod\limits_{u \neq n} e^{(b_u(k)) L_a(b_u(k))}}. \tag{53}$$

Moreover, (53) can be simplified using the Max-Log rule as follows

$$\begin{aligned} L_e(b_n(k)) = &\max_{\boldsymbol{\beta}_i \in \mathbb{S}_1^n} \frac{-\|\hat{\mathbf{x}}_k - \mathbf{u}_k\|_2^2}{\sigma_{k,v}^2} + \sum_{u \neq n} (b_u(k)) L_a(b_u(k)) \\ &- \max_{\boldsymbol{\beta}_i \in \mathbb{S}_0^n} \frac{-\|\hat{\mathbf{x}}_k - \mathbf{u}_k\|_2^2}{\sigma_{k,v}^2} + \sum_{u \neq n} (b_u(k)) L_a(b_u(k)). \end{aligned} \tag{54}$$

### *B. Proposed LC-VV-TDTE Detector*

In the MMSE-aided VV-TDTE detector, the filter coefficient $\mathbf{C}_k$ changes with $k$. This imposes an additional computational complexity. To tackle this issue, a low-complexity VV-TDTE detector that uses fixed filter coefficients is proposed in this section. The proposed detector works based on the following steps.

**Step 1:** Obtain the values of $\bar{\mathbf{s}}(k)$ and $\mathbf{V}(k)$ in (45) using (28) and (29), respectively, which is similar as step 1 of the proposed VV-TDTE detector.

**Step 2:** Apply SIC to the $k$-th GSM symbol. This step is also similar to the proposed VV-TDTE detector.

**Step 3:** Perform approximate MMSE detection.

In this step, the MMSE filter coefficients $\mathbf{C}$ are designed to be constant, and, as a result, the estimated signal turns

This article has been accepted for publication in a future issue of this journal, but has not been fully edited. Content may change prior to final publication. Citation information: DOI 10.1109/TWC.2017.2713777, IEEE Transactions on Wireless Communications



$$
\begin{aligned}
C_{\mathrm{S}} &= \underbrace{4N_rN_tNN^{'}K}_{step.2} + \underbrace{4N_rN_t^3NN^{'2}K + 4N_r^2N_t^2N^2N^{'}K + 2N^3N_r^3N_tK + 10N_r^2N_tN^2K + 4N_rN_tNK}_{step.3} \\
&+ \underbrace{N_uK2^{B+1}}_{Eq.(28)} + \underbrace{3N_uK2^{B+1} + 4N_uK}_{Eq.(29)} + \underbrace{4N_rN_tNK + 4N_t(L+1)K}_{Eq.(34)} + \underbrace{3KN_t2^B}_{Eq.(36)} \\
C_{\mathrm{V}} &= \underbrace{3N_uK2^{B+1} + 4N_uK}_{Eq.(29)} + \underbrace{4N_rN_t^2NN^{'2}K + 4N_r^2N_tN^2N^{'}K + 4N_r^2N_tN^2K + 2N^3N_r^3K + 6N^2N_r^2K}_{Eq.(46)} \\
&+ \underbrace{N_uK2^{B+1}}_{Eq.(28)} + \underbrace{4N_rN_tNN^{'}K}_{Eq.(47)} + \underbrace{4N_rN_tNK}_{Eq.(48)} + \underbrace{4N_rN_t^2NK + 4N_t^2K2^B}_{Eq.(50)} + \underbrace{2N_t^2K}_{Eq.(51)} + \underbrace{2N_t^2K}_{Eq.(52)} + \underbrace{(2N_t+1)K2^B}_{Eq.(54)} \\
C_{\mathrm{LC}} &= \underbrace{3N_uK2^{B+1} + 4N_uK}_{Eq.(29)} + \underbrace{4N_rN_tNN^{'}K}_{Eq.(47)} + \underbrace{4N_rN_tNK}_{Eq.(55)} + \underbrace{4N_rN_t^2NN^{'2} + 4N_r^2N_tN^2N^{'} + 4N_r^2N_tN^2 + 2N^3N_r^3 + 6N^2N_r^2}_{Eq.(60)} \\
&+ \underbrace{N_uK2^{B+1}}_{Eq.(28)} + \underbrace{4N_rN_t^2N + 4N_t^22^B}_{Eq.(61)} + \underbrace{2N_t^2}_{Eq.(62)} + \underbrace{2N_t^2NN_r + 4N_t^2NN_r(N+P-1) + 2N_t^3(N+P-1)}_{Eq.(63)} + \underbrace{(2N_t+1)K2^B}_{Eq.(54)}.
\end{aligned}
\tag{64}
$$

out to be based on an approximate implementation of the MMSE detection. In mathematical terms, we have

$$\hat{\mathbf{x}}_k = \mathbf{C}^H\mathbf{r}(k). \tag{55}$$

In the proposed VV-TDTE detector, in fact, the filter coefficients $\mathbf{C}$ are designed based on the coefficients $\mathbf{C}_k$. Since $\hat{\mathbf{V}}(k)$ changes with $k$, from (46) we evince that the coefficients $\mathbf{C}_k$ will vary with $k$, which introduces extra complexity. To further reduce the complexity of the proposed VV-TDTE detector, fixed filter coefficients $\mathbf{C}$ are employed in the proposed LC-VV-TDTE detector. Specifically, the coefficients $\mathbf{C}_k$ in (46) can be rewritten as

$$
\begin{aligned}
\mathbf{C}_k &= (\sigma_0^2\mathbf{I}_{(NN_r)} + \hat{\mathbf{H}}\hat{\mathbf{V}}(k)\hat{\mathbf{H}}^H)^{-1}\hat{\mathbf{H}}_{\mathbf{s}} \\
&= (\sigma_0^2\mathbf{I}_{(NN_r)} + \hat{\mathbf{H}}\mathbf{V}(k)\hat{\mathbf{H}}^H + \hat{\mathbf{H}}_{\mathbf{s}}(\mathbf{I}_{N_t} - \mathbf{V}_k^d)\hat{\mathbf{H}}_{\mathbf{s}}^H)^{-1}\hat{\mathbf{H}}_{\mathbf{s}}.
\end{aligned}
\tag{56}
$$

In the proposed LC-VV-TDTE detector, the fixed filter coefficients $\mathbf{C}$ are obtained using the time average of $\mathbf{C}_k$ as follows

$$\mathbf{C} = (\frac{1}{K}\sum_{k=1}^{K}(\sigma_0^2\mathbf{I}_{(NN_r)} + \hat{\mathbf{H}}\hat{\mathbf{V}}(k)\hat{\mathbf{H}}^H))^{-1}\hat{\mathbf{H}}_{\mathbf{s}}. \tag{57}$$

By substituting (56) in (57), we obtain

$$\mathbf{C} = (\sigma_0^2\mathbf{I}_{(NN_r)} + \frac{1}{K}\sum_{k=1}^{K}\hat{\mathbf{H}}\mathbf{V}(k)\hat{\mathbf{H}}^H - \hat{\mathbf{H}}_{\mathbf{s}}\left(\mathbf{I}_{N_t} - \mathbf{V}_k^d\right)\hat{\mathbf{H}}_{\mathbf{s}}^H)^{-1}\hat{\mathbf{H}}_{\mathbf{s}}. \tag{58}$$

In order to ensure that $\hat{\mathbf{x}}_k$ is independent of $L_a(b_n(k))$, we set the elements of $L_a(b_n(k))$ to zero when computing $\hat{\mathbf{x}}_k$, which yields $\bar{\mathbf{x}}_k = \mathbf{0}_{N_t\times 1}$ and $\mathbf{v}_k = \mathbf{1}_{N_t\times 1}$. As a consequence, the term $\sum_{k=1}^{K}\hat{\mathbf{H}}\mathbf{V}(k)\hat{\mathbf{H}}^H - \hat{\mathbf{H}}_{\mathbf{s}}\left(\mathbf{I}_{N_t} - \mathbf{V}_k^d\right)\hat{\mathbf{H}}_{\mathbf{s}}^H$ in $\mathbf{C}$ simplifies as follows

$$
\begin{aligned}
&\sum_{k=1}^{K}\hat{\mathbf{H}}\mathbf{V}(k)\hat{\mathbf{H}}^H - \hat{\mathbf{H}}_{\mathbf{s}}\left(\mathbf{I}_{N_t} - \mathbf{V}_k^d\right)\hat{\mathbf{H}}_{\mathbf{s}}^H \\
&= K\hat{\mathbf{H}}\hat{\mathbf{V}}\hat{\mathbf{H}}^H,
\end{aligned}
\tag{59}
$$

where $\hat{\mathbf{V}} = \mathsf{diag}(\hat{\mathbf{v}}^T, ..., \hat{\mathbf{v}}^T, ..., \hat{\mathbf{v}}^T)$ with $\hat{\mathbf{v}} = \frac{1}{K}\sum_{k=1}^{K}\mathbf{v}_k$.

By substituting (59) in (58), we obtain

$$\mathbf{C} = (\sigma_0^2\mathbf{I}_{(NN_r)} + \hat{\mathbf{H}}\hat{\mathbf{V}}\hat{\mathbf{H}}^H)^{-1}\hat{\mathbf{H}}_{\mathbf{s}}. \tag{60}$$

**Step 4** Calculate the LLRs. The CPDF of the proposed LC-VV-TDTE detector is based on (49), where $\mathbf{u}_k$ and $\sigma_{k,v}^2$ are calculated as follows

$$
\begin{aligned}
\mathbf{u}_k &= E(\hat{\mathbf{x}}_k\,|\mathbf{x}_k = \boldsymbol{\beta}_i) \\
&= \mathbf{C}^H E(\mathbf{y}(k) - \hat{\mathbf{H}}\hat{\mathbf{s}}(k))\,|\mathbf{x}_k = \boldsymbol{\beta}_i) \\
&= \mathbf{C}^H\hat{\mathbf{H}}_{\mathbf{s}}\boldsymbol{\beta}_i,
\end{aligned}
\tag{61}
$$

and

$$\sigma_{k,v}^2 = \|\mathbf{Cov}(\hat{\mathbf{x}}_k, \hat{\mathbf{x}}_k\,|\mathbf{x}_k = \boldsymbol{\beta}_i)\|_2, \tag{62}$$

where

$$
\begin{aligned}
&\mathbf{Cov}(\hat{\mathbf{x}}_k, \hat{\mathbf{x}}_k\,|\mathbf{x}_k = \boldsymbol{\beta}_i) \\
&= \mathbf{C}^H(\sigma_0^2\mathbf{I}_{NN_r} + \hat{\mathbf{H}}\hat{\mathbf{V}}\hat{\mathbf{H}}^H - \hat{\mathbf{V}}^d\hat{\mathbf{H}}_{\mathbf{s}}\hat{\mathbf{H}}_{\mathbf{s}}^H)\mathbf{C} \\
&= \sigma_0^2\mathbf{C}^H\mathbf{C} + \mathbf{C}^H\hat{\mathbf{H}}\mathbf{V}^{'}\hat{\mathbf{H}}^H\mathbf{C},
\end{aligned}
\tag{63}
$$

where we have $\mathbf{V}^{'} = \mathsf{diag}(\underbrace{\hat{\mathbf{v}}^T, ..., \hat{\mathbf{v}}^T}_{1\times(P+N_2-1)N_t}, \mathbf{0}_{N_t\times 1}^T, \underbrace{\hat{\mathbf{v}}^T, ..., \hat{\mathbf{v}}^T}_{1\times N_1N_t})$ and $\hat{\mathbf{V}}^d = \mathsf{diag}(\hat{\mathbf{v}})$. Finally, based on the estimated $\hat{\mathbf{x}}_k$ in (55), $\mathbf{u}_k$ in (61), $\sigma_{k,v}^2$ in (62), the *priori* LLRs, and the extrinsic information LLRs of the encoded bits are obtained from (54).

### C. Computational Complexity Analysis

In this section, the complexity order of the proposed detectors are analyzed in terms of real-valued multiplications. The complexity order of PIC-R-SIC-aided TDTE and M-algorithm-aided TDTE detectors are available in [34]. The complexity order of the SC-FDE detector can be found in [25]. Let us consider the matrices $\mathbf{A} \in \mathbb{C}^{m\times n}$, $\mathbf{B} \in \mathbb{C}^{n\times p}$, and $\mathbf{C} \in \mathbb{C}^{n\times 1}$. The computation of $\mathbf{AB}$ and $\|\mathbf{C}\|_2^2$ requires $4mnp$ and $2n$ real-valued multiplications, respectively. The complexity order of the proposed TDTE detectors are summarized, in terms of real-valued multiplications, in (64), where $N^{'} = N + P - 1$, $C_{\mathrm{S}}$, $C_{\mathrm{V}}$, $C_{\mathrm{LC}}$ are referred to SS-TDTE, VV-TDTE, LC-VV-TDTE, respectively. As a benchmarker, the complexity of the MAP-SD detector is computed as

$$
\begin{aligned}
C_{\mathrm{MAP-SD}} &= \underbrace{2^BK + 4N_rP2^BK + 2^{BP}(2N_r+2)K}_{\text{Complexity of } \gamma_k(s,s')} \\
&+ \underbrace{4\cdot 2^{BP}K}_{\text{Complexity of } \alpha_k(s)} + \underbrace{4\cdot 2^{BP}K}_{\text{Complexity of } \beta_{k+1}(s)}.
\end{aligned}
\tag{65}
$$

This article has been accepted for publication in a future issue of this journal, but has not been fully edited. Content may change prior to final publication. Citation information: DOI 10.1109/TWC.2017.2713777, IEEE Transactions on Wireless Communications



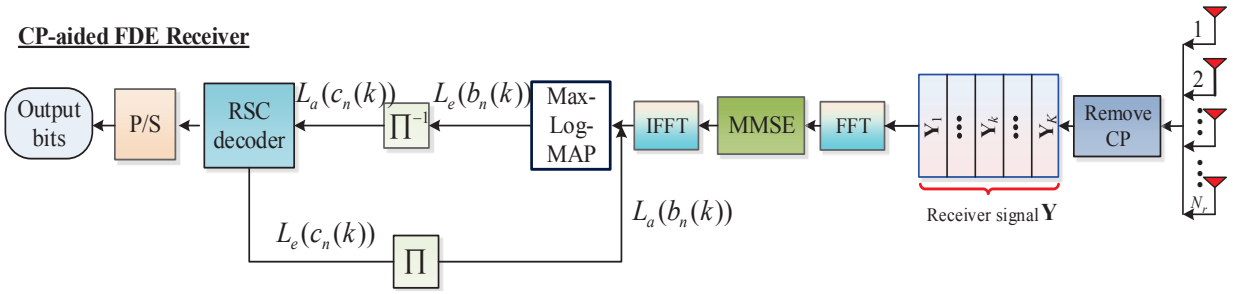


Fig. 2. Classical SoD-aided SC-FDE detector for CP-SC-GSM systems.

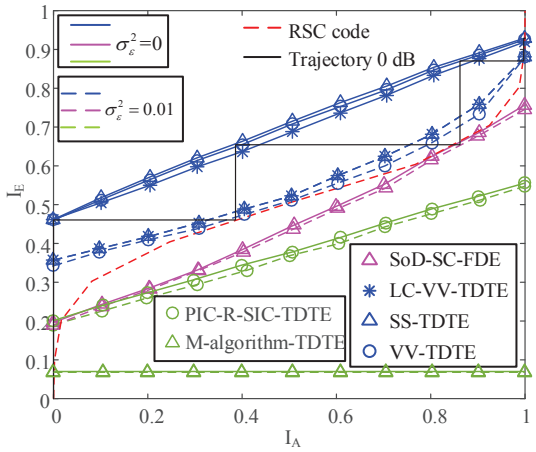


Fig. 3. EXIT chart comparison of several TDTE detectors for the QPSK-aided ZP-SC-GSM system with an interleaver length of 40,960 bits, and $N_t = 4$, $N_r = 4$, $N_u = 1$, $K = 256$, $P = 15$, and $L = 4$ for SNR=0 dB. The EXIT chart of the SoD-aided SC-FDE detector for the corresponding CP-SC-GSM system is also plotted for comparison. The EXIT trajectory of the proposed VV-TDTE detector is drawn at SNR=0 dB.

## V. EXIT Chart Performance Analysis

### *A. EXIT Chart Performance comparisons and Convergence Behavior Analysis*

Based on the structure of the two-stage concatenated RSC-coded ZP-SC-GSM transceiver in Fig. 1, the EXIT chart performances and convergence behaviors of the proposed TDTE detectors are analyzed and compared in perfect and imperfect channel estimation. For comparative purpose, the EXIT chart performances of the two-stage concatenated RSC-coded CP-SC-GSM system of Fig. 2 are added. In this section, both ZP-SC-GSM and CP-SC-GSM systems employ RSC (2,1,2) code with the octal generate polynomial $(G_r, G) = (7, 5)_8$ and the interleaver length of 40,960 bits having $K = 256$, $P = 15$, and $P-1$ CP and ZP lengths. For the imperfect channel estimation, according to [41], we consider the estimated channel with a fixed error variance $\sigma_\varepsilon^2$ as follows

$$\mathbf{H}_{P-1,e} = \mathbf{H}_{P-1} + \mathbf{H}_{P-1}^e, ....\mathbf{H}_{0,e} = \mathbf{H}_0 + \mathbf{H}_0^e, \qquad (66)$$

where $\mathbf{H}_p^e, p = [0, ..., P-1]$ denote the channel estimation error, whose elements follow a complex Gaussian distribution of $\mathcal{CN}\left(0, \sigma_\varepsilon^2\right)$. For perfect channel estimation, we have $\sigma_\varepsilon^2 = 0$. Additionally, in these configurations, the value of $K$ and $P$ is large, so that the ML-aided and MAP-SD-aided TDTE detectors become impractical to be compared due to its intractable complexity.

Fig. 3 portrays the EXIT chart performance of the QPSK-aided ZP-SC-GSM and CP-SC-GSM systems having $N_t = N_r = 4$, $N_u$=1 at signal-to-noise ratio (SNR) of 0 dB, where the SNR refers to the ratio of the transmit symbol power to the noise power. Observed from Fig. 3 that, for the perfect channel estimation, all the proposed SS-TDTE, VV-TDTE and LC-VV-TDE detectors provide more extrinsic information than the conventional TDTE detectors, such as the PIC-R-SIC, the M-algorithm and the classical SoD-aided SC-FDE detectors. This implies that the ZP-SC-GSM system with the proposed TDTE detectors outperform ZP-SC-GSM system with the conventional TDTE detectors and CP-SC-GSM system with the SoD-aided SC-FDE detector in terms of BER. It's also shown that the proposed SS-TDTE, VV-TDTE and LC-VV-TDTE detectors offer similar EXIT chart performances, which implies that the proposed TDTE detectors can provide nearly the same BER performance for the considered system configurations. The similar trend can be observed for the case of imperfect channel estimation with $\sigma_\varepsilon$=0.01. Furthermore, we plot the EXIT trajectory of the proposed VV-TDTE detector at SNR=0 dB using Monte-Carlo simulations as well as the EXIT curve of the RSC (2,1,2) code, where the corresponding EXIT trajectory reaches convergence point of $(I_\mathrm{A}, I_\mathrm{E}) = (1, 0.93)$ after $I_\mathrm{iter} = 4$ iterations.

Next, Fig. 4 illustrates the EXIT chart performance and convergence behaviors of the proposed TDTE detectors under the unbalanced antenna configurations ($N_t = 8, N_r = 4, N_u = 1$). As noted in Section II-C, the PIC-R-SIC-aided and M-algorithm-aided TDTE detectors perform poorly with such configurations. As a result, their EXIT charts are not shown in Fig. 4. For further comparison, the EXIT charts of the CP-SC-GSM system with SoD-aided SC-FDE detection are added. The analysis is performed by varying the SNR from -2 dB to 2 dB for perfect channel estimation and -1 dB to 3 dB for imperfect channel estimation. The EXIT trajectories of the proposed TDTE detectors at SNR=1 dB for perfect channel estimation and at SNR=3 dB for imperfect channel estimation are also plotted.

As can be seen from Fig. 4, for the perfect channel estimation, the EXIT trajectories of 1 dB reach convergence points of the proposed SS-TDTE , VV-TDTE, and LC-VV-TDTE detectors of $(I_\mathrm{A}, I_\mathrm{E}) = (1, 0.95)$ after $I_\mathrm{iter} = 4$ iterations. For the case of imperfect channel estimation, due to the inaccurate channel estimation, the EXIT trajectories of 3 dB can reach convergence points of the proposed SS-TDTE , VV-TDTE, and LC-VV-TDTE detectors of $(I_\mathrm{A}, I_\mathrm{E}) = (1, 0.95)$ after $I_\mathrm{iter} = 4$ iterations. Moreover, as shown in Fig. 4 the proposed SS-TDTE, VV-TDTE and LC-VV-TDE detectors can provide more extrinsic information than the classical SoD-aided SC-

This article has been accepted for publication in a future issue of this journal, but has not been fully edited. Content may change prior to final publication. Citation information: DOI 10.1109/TWC.2017.2713777, IEEE Transactions on Wireless Communications



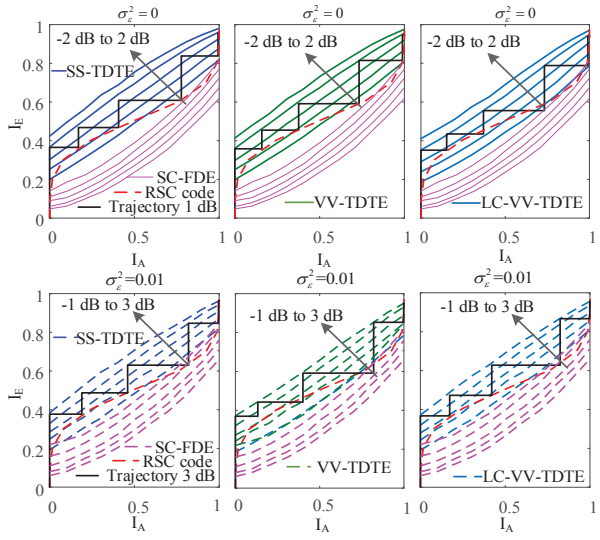


Fig. 4. EXIT charts of the proposed TDTE detectors for the QPSK-aided ZP-SC-GSM system with an interleaver length of 40,960 bits, and $N_t = 8$, $N_r = 4$, $N_u = 1$, $K = 256$, $P = 15$, and $L = 4$. The EXIT charts of the SoD-aided SC-FDE detector for the corresponding CP-SC-GSM system is also plotted for comparison.

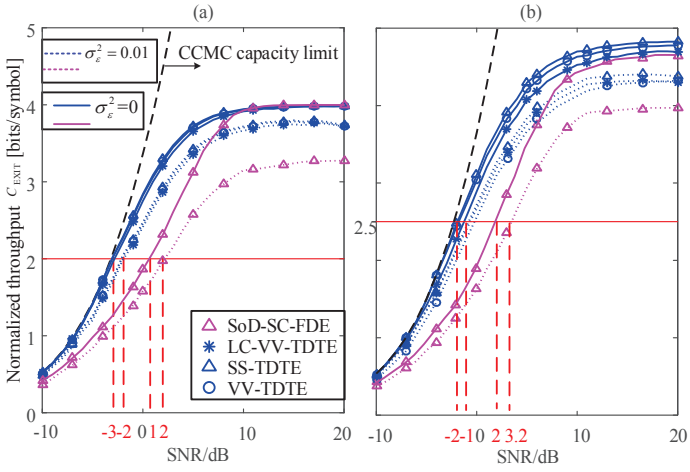


Fig. 5. Maximum achievable limit of the proposed TDTE detectors based ZP-SC-GSM system and that of the SoD-aided SC-FDE based CP-SC-GSM system with an interleaver length of 40,960 bits. a) $N_t = 4$, $N_r = 4$, $N_u = 1$, $K = 256$, $P = 15$, $L = 4$ and $R_{\text{GSM}} = 4$ bits/symbol; b) $N_t = 8$, $N_r = 4$, $N_u = 1$, $K = 256$, $P = 15$, $L = 4$ and $R_{\text{GSM}} = 5$ bits/symbol.

FDE detectors for both perfect and imperfect channel estimation under this unbalanced antenna configuration.

### B. Maximum Achievable Limit

In this section, the maximum achievable limit of the coded ZP-SC-GSM system with the proposed TDTE detectors is shown in Fig. 5 based on the EXIT chart [30]. The analysis assumes the same configuration as in Figs. 3 and 4. According to [30], it is a challenging task to derive the theoretical limit of the SoD detector. As such, the maximum achievable limit obtained by the EXIT chart can be used to reveal the limit of the SoD detectors. Moreover, the coded ZP-SC-SM system in Fig. 5 has a long channel impulse response, so that the theoretical limit of the optimal detector is not attainable due to its intractable complexity. For comparative purposes, the maximum achievable limit of the CP-SC-GSM system with the SoD-aided FDE detector and the associated capacity of the continuous input continuous-output memoryless channel (CCMC) are added as benchmarkers. The maximum achievable limit is calculated as [30]: $C_{\text{EXIT}} = \mathcal{A}(\rho)R_{\text{GSM}}$ bits/symbol, where $0 < \mathcal{A}(\rho) < 1$ represents the area under the EXIT curve at SNR$= \rho$ and $R_{\text{GSM}}$ is the transmission rate of GSM symbols. Hence, given SNR $= \rho$, the more extrinsic information the detector can provide, the larger $\mathcal{A}(\rho)$ is, resulting in larger $C_{\text{EXIT}}$. For imperfect channel estimation, there may exist a incur BER error floor at high SNRs, so that the value of $\mathcal{A}(\rho)$ can not approach one, leading to lower $C_{\text{EXIT}}$.

As can be seen from Fig. 5, when employing a half-rate RSC code for the ZP-SC-GSM and CP-SC-GSM systems, the transmission rates are 2 and 2.5 bits/symbol for the antenna configurations of $N_t = 4$, $N_r = 4$ and $N_t = 8$, $N_r = 4$, respectively. For the case of $N_t = 4$ and $N_r = 4$, the limit of the proposed SS-TDTE detector-aided ZP-SC-GSM is reached when $\rho = -3$ dB for $\sigma_\varepsilon^2 = 0$ and $\rho = -2$ dB for $\sigma_\varepsilon^2 = 0.01$. For the configuration of $N_t = 8$ and $N_r = 4$, this capacity limit is reached when $\rho = -2$ dB for $\sigma_\varepsilon^2 = 0$ and $\rho = -1$ dB for $\sigma_\varepsilon^2 = 0.01$. Moreover, the ZP-SC-GSM systems with the proposed TDTE detectors are capable of achieving a lower maximum achievable limit than the CP-SC-GSM system with the SoD-aided FDE detector and approaching the CCMC capacity limit under both the balanced and unbalanced antenna configurations.

## VI. Simulation Results

In this section, the BER performance of the proposed detectors for application to ZP-SC-GSM is presented and compared. The RSC (2,1,2) code with octal generator polynomial equal to $(G_r, G) = (7, 5)_8$ is employed. The CP and ZP lengths are equal to $P-1$. The interleaver lengths are selected based on the specific antenna configurations.

### A. Performance and Complexity Comparisons for the ZP-SC-GSM Systems with Different TDTE Detectors

Fig. 6 compares the BERs of various TDTE detectors for the BPSK-aided ZP-SC-GSM system with $N_t = 2$, $N_r = 2$, $N_u = 1$, $P = 3$, and different values of $K$ and interleaver lengths. The corresponding complexity comparisons are shown in Fig. 7. As can be observed from Figs. 6 (a) and 7, the ML-aided TDTE detector achieves the optimal BER performance albeit with the highest complexity. For the case of $K = 256$ and $K = 512$, the complexity orders of the ML-aided TDTE detector are larger than $2^{256}$ and $2^{512}$, respectively, resulting in impractical implementation. Hence the performance and complexity of the ML-aided TDTE detector are not shown in Figs. 6 (b) and (c), and we adopt the MAP-SD detector described in Section II-A as a benchmarker.

As can be seen from Figs. 6 and 7, the proposed TDTE detectors have similar BER performance, while the proposed LC-VV-TDTE detector has the lowest complexity. Compared to the conventional M-algorithm-aided and PIC-R-SIC TDTE detectors, the proposed TDTE detectors are able to provide considerable performance gains with a 99% reduction in complexity. As shown in Fig. 6 (b), the non-linear MAP-SD based detector preforms better than the proposed linear TDTE detectors, when the interleaver length is small, e.g., 1024 bits. However, for the case of $K = 256$ with a larger interleaver length of 10,240

This article has been accepted for publication in a future issue of this journal, but has not been fully edited. Content may change prior to final publication. Citation information: DOI 10.1109/TWC.2017.2713777, IEEE Transactions on Wireless Communications



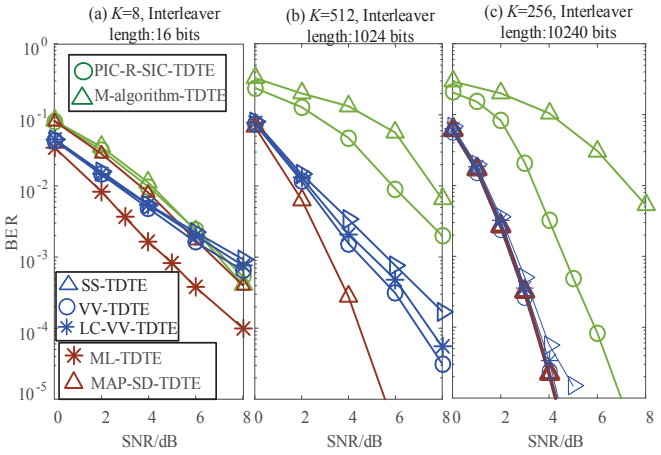


Fig. 6. BER performance comparison among various TDTE detectors for the BPSK-aided ZP-SC-GSM system with $N_t = 2$, $N_r = 2$, $N_u = 1$, $P = 3$ having different value of $K$. The number of iterations is $I_{\text{iter}} = 2$.

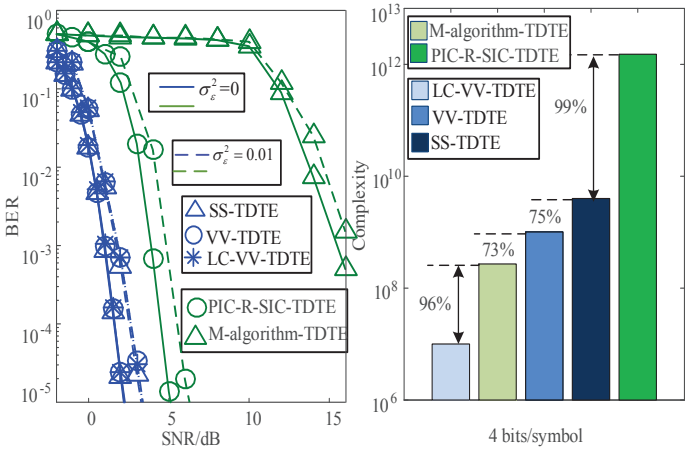


Fig. 8. Performance and complexity comparison among various detectors for the QPSK-aided ZP-SC-GSM system with an interleaver length of 40,960 bits, $N_t = 4$, $N_r = 4$, $N_u = 1$, $K = 256$, $P = 15$, and $L = 4$. The number of iterations is $I_{\text{iter}} = 2$.

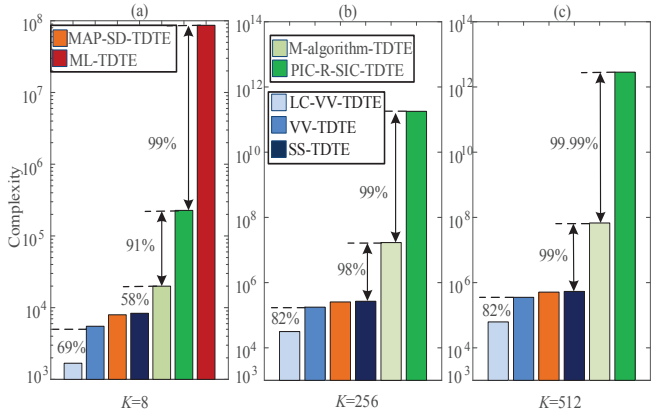


Fig. 7. Complexity comparison among various TDTE detectors for the BPSK-aided ZP-SC-GSM system with $N_t = 2$, $N_r = 2$, $N_u = 1$, $P = 3$ having different value of $K$; a) $K = 8$; b) $K = 256$; c) $K$=512.

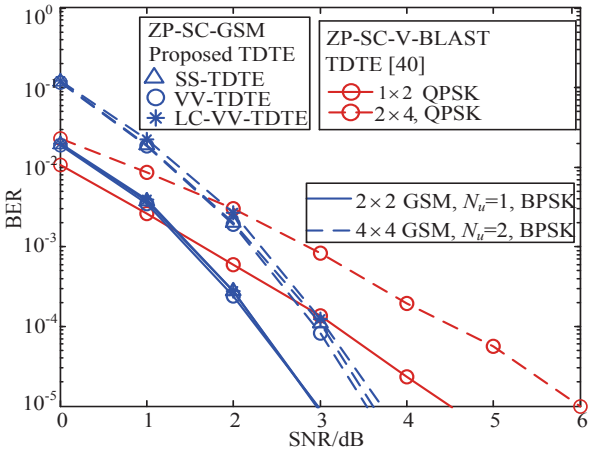


Fig. 9. Performance comparison between ZP-SC-GSM and ZP-aided SC V-BLAST systems with an interleaver length of 40,960 bits, and $K = 256$, $P = 15$, and $L = 4$. The number of iterations is $I_{\text{iter}} = 2$.

bits consisting of 20 data frames, the proposed LC-VV-TDTE detector is capable of approaching the MAP-SD detector with a 80% reduction in complexity.

Next, Fig. 8 compares the BER performance and complexity of various TDTE detectors for the QPSK-aided ZP-SC-GSM systems with $N_t = 4$, $N_r = 4$, $N_u = 1$, $K = 256$, $P = 15$, and an interleaver length of 40,960 bits. In this case, the ML-aided TDTE and MAP-SD TDTE detectors become impractical. As shown in Fig. 8, the proposed TDTE detectors outperform the PIC-R-SIC-aided TDTE and $M$-algorithm-aided TDTE detectors by 3 dB and 14 dB at the BER=$10^{-3}$ with more than 99% reduction in complexity. The similar trend can be observed for the case of imperfect channel estimation with $\sigma_\varepsilon$=0.01. In summary, the proposed TDTE detectors are capable of striking an elegant balance between the BER performance and complexity for the ZP-SC-GSM system with large values of $K$, $B$ and $P$.

### *B. Performance Comparisons Between ZP-SC-GSM and ZP-SC-VBLAST Systems*

Fig. 9 compares the performance of the proposed TDTE detectors based ZP-SC-GSM system with the conventional TDTE detector [38] based ZP-SC-V-BLAST system. Specifically, we employ BPSK-aided $2 \times 2$ SM (GSM, $N_u = 1$) and QPSK-aided $1 \times 2$ V-BLAST to obtain the same normalized throughput of 2 bps/Hz. We also employ BPSK-aided $4 \times 4$ GSM with $N_u = 2$ and QPSK-aided $2 \times 4$ V-BLAST to obtain the same normalized throughput of 3bps/Hz. At high SNRs, as can be observed from Fig. 9, ZP-SC-GSM with the proposed TDTE detectors exhibit better BER performance than its ZP-SC-V-BLAST counterpart that uses the TDTE detector in [38].

### *C. Performance Comparisons Between ZP-SC-GSM and CP-SC-GSM Systems*

Figs. 10 and 11 plot the BER performance of the ZP-SC-GSM system with the proposed TDTE detectors and $I_{\text{iter}} = 4$ iterations under perfect channel estimation ($\sigma_\varepsilon^2 = 0$) and imperfect channel estimation ($\sigma_\varepsilon^2 = 0.01$). Moreover, the antenna configuration is the same as in Figs. 4 and 5. For comparative purposes, the BER of the CP-SC-GSM scheme with the SoD-aided SC-FDE detector is also shown. As shown in Figs. 10 and 11, the ZP-SC-GSM system with the proposed TDTE detectors is able to provide a performance gain around 4 dB as opposed to the SoD-aided SC-FDE based CP-SC-GSM system

This article has been accepted for publication in a future issue of this journal, but has not been fully edited. Content may change prior to final publication. Citation information: DOI 10.1109/TWC.2017.2713777, IEEE Transactions on Wireless Communications



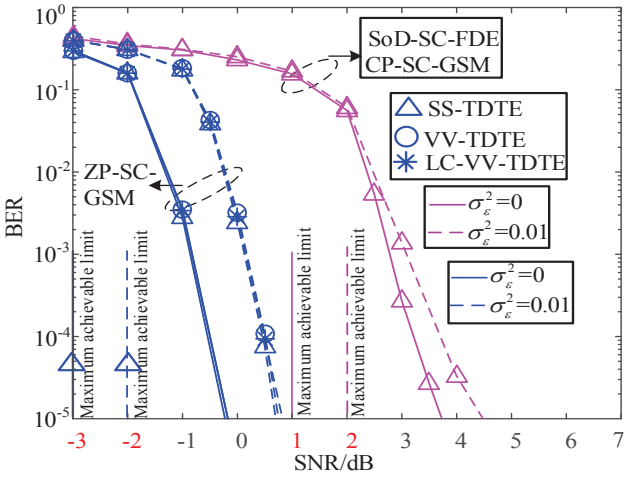


Fig. 10. Performance comparison among various detectors for the QPSK-aided ZP-SC-GSM and CP-SC-GSM systems with an interleaver length of 40960 bits, and $N_t = 4$, $N_r = 4$, $N_u = 1$ $K = 256$, $P = 15$, and $L = 4$. The number of iterations is $I_{\text{iter}} = 4$.

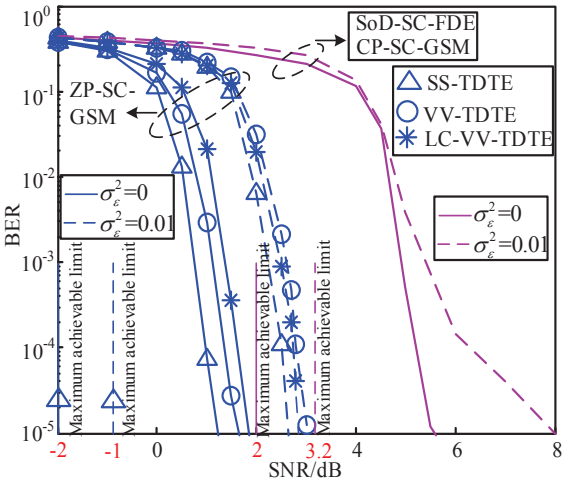


Fig. 11. Performance comparison among various detectors for the QPSK-aided ZP-SC-GSM systems with an interleaver length of 40,960 bits, and $N_t = 8$, $N_r = 4$, $N_u = 1$, $K = 256$, $P = 15$, and $L = 4$. The number of iterations is $I_{\text{iter}} = 4$.

with $N_t = N_r = 4$ and $N_t = 8, N_r = 4$, under both perfect channel estimation ($\sigma_\varepsilon^2 = 0$) and imperfect channel estimation ($\sigma_\varepsilon^2 = 0.01$). Furthermore,it is also revealed that the proposed TDTE detectors can approach to the maximum achievable limit after four iterations as shown in Figs. 10 and 11.

Finally, Fig. 12 compares the BER performance of the proposed TDTE-aided ZP-SC-GSM and SoD-SC-FDE-aided CP-SC-GSM system having $N_t = 32$, $N_r = 16$, $K = 64$, $P = 15$ and $L = 4$ under perfect channel estimation ($\sigma_\varepsilon^2 = 0$) and imperfect channel estimation with $\sigma_\varepsilon^2 = 0.01$. It is noted that the ZP-SC-GSM system with the proposed TDTE detectors outperforms its CP-SC-GSM counterpart with the SoD-aided SC-FDE detector by around 6 dB at BER=$10^{-5}$ for both mentioned channel estimation scenarios. Moreover, observed from Figs. 11 and 12, the proposed VV-TDTE detector is more sensitive to the estimated channel error than its LC-VV-TDTE counterpart. This can be explained that the MMSE filter coefficient in the proposed LC-VV-TDTE detector is approximately calculated. When the imperfect channel estimation is considered, the MMSE filter coefficients in proposed VV-TDTE and LC-VV-TDTE detectors are both approximately calculated. In this case, the proposed LC-VV-TDTE detector become less sensitive than its VV-TDTE counterpart.

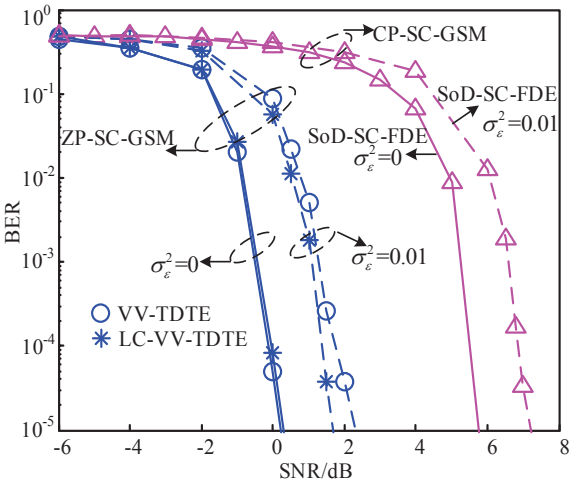


Fig. 12. Performance comparison among various detectors for the QPSK-aided ZP-SC-GSM systems with an interleaver length of 53,760 bits, and $N_t = 32$, $N_r = 16$, $K = 64$, $P = 15$, and $L = 4$. The number of iterations is $I_{\text{iter}} = 2$.

## VII. Conclusion

This paper introduced low-complexity TDTE detectors for application to ZP-SC-GSM systems. We generalized the conventional hard-decision time domain detectors to the TDTE detectors. To further improve their performance, we proposed three low-complexity TDTE detectors based on the SIC-aided MMSE principle and for application to ZP-aided GSM-SC systems. With respect to known detection schemes, simulation results show that the proposed detectors are capable of achieving considerable performance gains with a reduced decoding complexity. In particular, the ZP-SC-GSM system based upon the proposed TDTE detectors is able to provide a considerable performance gain against the classic FDE-based CP-SC-GSM system and conventional TDTE-based ZP-SC-V-BLAST system, especially for unbalanced antenna configurations.

## References

[1] A. Younis, N. Serafimovski, R. Mesleh, and H. Haas, "Generalised spatial modulation," in *Proc. 2010 IEEE Signal System and Computers*, Pacific Grove, Nov. 2010, pp. 1498-1502.

[2] J. L. Fu, C. P. Hou, W. Xiang, L. Yan, and Y. H. Hou, "Generalised spatial modulation with multiple active transmit antennas," *in Proc. 2010 IEEE GLOBECOM Workshops*, pp. 839-844.

[3] L. Xiao, P. Yang, Y. Xiao, S. Fan, M. D. Renzo, W. Xiang, and S. Li, "Efficient Compressed Sensing Detectors for Generalized Spatial Modulation Systems," *IEEE Trans. Veh. Technol.*, vol. PP, no. 99, pp. 1-1, April. 2016. (doi: 10.1109/TVT.2016.2558205).

[4] R. Mesleh, H. Haas, S. Sinanovic, C. W. Ahn, and S. Yun, "Spatial modulation," *IEEE Trans. Veh. Technol.*, vol. 57, no. 4, pp. 2228-2241, Jul. 2008.

[5] P. Yang, M. Di Renzo, Y. Xiao, S. Q. Li, and L. Hanzo, "Design guidelines for spatial modulation," *IEEE Commun. Surveys Tuts.*, vol. 17, no. 1, pp. 6-26, First Quart., 2015.

[6] Rakshith Rajashekar, K.V.S. Hari, and Lajos Hanzo, "Reduced-complexity ML detection and capacity-optimized training for spatial modulation systems," *IEEE Transactions on Communications*, vol. 62, no. 1, pp. 112- 125, Jan. 2014.

[7] A. Stavridis, S. Sinanovic, M. Di Renzo, and H. Hass, "Energy evaluation of spatial modulation at a multi-antenna base station," in Proc *IEEE Veh. Technol. Conf. Fall*, Las Vegas, Sept. 2013, pp. 1-5.

[8] N. Serafimovski, A. Younis, R. Mesleh, M. Di Renzo, C. X. Wang, P. M. Grant, and H. Haas, "Practical implementation of spatial modulation," *IEEE Trans. Veh. Technol.*, vol. 62, no. 9, pp. 4511-4523, Nov. 2013.

[9] K. Ishibashi and S. Sugiura, "Effects of antenna switching on band-limited spatial modulation," *IEEE Wireless Commun. Lett.,* vol. 3, no. 4, pp. 345-348, Apr. 2014.

[10] P. Wolniansky, G. Foschini, G. Golden, and R. Valenzuela, "V-BLAST: anarchitecture for realizing very high data rates over the rich-scattering wireless channel," in *Proc. 1998 International Symp. Signals, Syst., Electron.*, Pisa, Oct. 1998, pp. 295-300.

[11] S. M. Alamouti, "A simple transmitter diversity scheme for wireless communications," *IEEE J. Select. Areas Commun.*, vol. 16, no. 8, pp. 1451-1458, Oct. 1998.

[12] P. Raviteja, T. L. Narasimhan, and A. Chockalingam, "Multiuser SM-MIMO versus massive MIMO: Uplink performance comparison," in *Proc. IEEE Information Theroy and Applications Workshop*, San Diego, CA, Feb. 2014, pp. 1-7.

[13] T. Lakshmi Narasimhan, Student Member, IEEE, P. Raviteja, and A. Chockalingam, "Generalized spatial modulation in large-scale multiuser MIMO systems," *IEEE Trans. Wireless Commun.*, vol. 14, no. 7, pp. 3764-3779, Jul. 2015.

[14] P. Yang, Y. Xiao, L. Li, Q. Tang, and S. Q. Li, "Link adapation for spatial modulation with limited feedback," *IEEE Trans. Veh. Technol.*, vol. 61, no. 8, pp. 3808-3813, Oct. 2012.

[15] Rakshith Rajashekar, K.V.S. Hari, and Lajos Hanzo, "Antenna selection in spatial modulation systems," *IEEE Commun. Lett.*, vol. 17, no. 3, pp. 521-524, Mar. 2013.

[16] Rakshith Rajashekar, K.V.S. Hari, and Lajos Hanzo, "Quantifying the transmit diversity order of Euclidean distance based antenna selection in spatial modulation," *IEEE Sig. Process. Lett.*, vol. 22, no. 9, pp. 1434- 1437, Sep. 2015.

[17] P. Yang, Y. Xiao, B. Zhang, S. Q. Li, M. El-Hajjar, and L. Hanzo, "Star-QAM signaling constellations for spatial modulation," *IEEE Trans. Veh. Technol.*, vol. 63, no. 8, pp. 3741-3749, Oct. 2014.

[18] P. Yang, B. Zhang, Y. Xiao, B. Dong, and S. Q. Li, "Detected-and-forward relaying aided cooperative spatial modulation for wireless networks," *IEEE Trans. Commun.*, vol. 61, no. 11, pp. 4500-4511, Nov. 2013.

[19] C. Xu, S. Sugiura, S. X. Ng, and L. Hanzo, "Spatial modulation and space time shift keying: optimal performance at a reduced detection complexity," *IEEE Trans. Commun.*, vol. 61, no. 1, Jun. 2013. pp. 1144-1153, Apr. 2011.

[20] C. Xu, S. Sugiura, S. X. Ng, and L. Hanzo, "Reduced-complexity soft-decision aided space-time shift keying,"*IEEE Signal Proc. Lett.*, vol. 18, no. 10, pp. 547-550, Oct. 2011.

[21] P. Yang, Y. Xiao, L. Dan, and S. Li, "An improved matched-filter based detection algorithm for space-time shift keying systems," *IEEE Signal Proc. Lett.*, vol. 19, no. 5, pp. 271-274, May 2012.

[22] L. Xiao, P. Yang, Y. Xiao, J. Liu, S. Fan, B. Dong, and S. Li, "An improved soft-input soft-output detector for generalized spatial modulation," *IEEE Signal Proc. Lett.,* vol. 23, no. 1, pp. 30-34, Jan. 2016.

[23] S. Ganesan, R. Mesleh, H. Haas, C. W. Ahn, and S. Yun, "On the performance of spatial modulation OFDM," in *in Proc. 2006 IEEE Signal System and Computers*, Pacific Grove, CA, Nov. 2006, pp. 1825-1829.

[24] M. L. Kadir, S. Sugiura, J. Zhang, S. Chen, and L. Hanzo, "OFDMA/SC-FDMA aided space-time shift keying for dispersive multiuser scenarios," *IEEE Trans. Veh. Technol.*, vol. 62, no. 1, pp. 408-414, Jan. 2013.

[25] P. Yang, Y. Xiao, Y. L. Guan, K. V. S. Hari, A. Chockalingam, S. Sugiura, H. Haas, M. Di Renzo, C. Masouros, Z. Liu, L. Xiao, S. Li, and L. Hanzo, "Single-carrier spatial modulation: A promising design for large-scale broadband antenna systems," *IEEE Commun. Surveys Tuts.*, vol. 18, no. 3, pp. 1687-1716, Feb. 2016.

[26] H. A. Ngo, C. Xu, S. Sugiura, and L. Hanzo, "Space-time-frequency shift keying for dispersive channels," *IEEE Singal Proc. Lett.*, vol. 18, no. 3, pp. 177-180, Mar. 2011.

[27] P. Som and A. Chockalingam, "Spatial modulation and space shift keying in single carrier communication," in *Proc. IEEE PIMRC*, Sydney, NSW, Sept. 2012, pp. 1962-1967.

[28] S. Wang, Y. Li, M. Zhao, and J. Wang, "Energy efficient and low-complexity uplink transceiver for massive spatial modulation MIMO," *IEEE Trans. Veh. Technol.*, vol. 64, no. 10, pp. 4617-4632, Oct. 2015.

[29] S. Wang, Y. Li, and J. Wang, "Multiuser detection in massive spatial modulation MIMO with low-resolution ADCs," *IEEE Trans. Wireless Commun.*, vol. 14, no. 4, pp. 2156-2168, Apr. 2015.

[30] S. Sugiura and L. Hanzo, "Single-RF spatial modulation requires single-carrier transmission: frequency-domain turbo equalization for dispersive channels," *IEEE Trans. Veh. Technol.*, vol. 64, no. 10, pp. 4870-4875, Oct. 2015.

[31] R. Rajasherkar, K. V. S. Hari, and L. Hanzo, "Spatial modulation aided zero-padded single carrier transmission for dispersive channels," *IEEE Trans. Commun.*, vol. 61, no. 6, pp. 2318-2329, June 2013.

[32] R. Rajasherkar, K. V. S. Hari, and L. Hanzo, "A reduced-complexity partial-interference-cancellation group decoder for STBCs," *IEEE Sig. Proc. Lett.*, vol. 20, no. 10, pp. 929 - 932, Oct. 2013.

[33] L. Xiao, P. Yang, Y. Zhao, Y. Xiao, J. Liu, and S. Li,"Low-complexity tree search-based detection algorithms for generalized spatial modulation aided single carrier systems," in *Proc. IEEE 2016 ICC.*, Malaysia, May, 2016.

[34] L. Xiao, L. Dan, Y. Zhang, Y. Xiao, P. Yang, and S. Li, "A low-complexity detection scheme for generalized spatial modulation aided single carrier systems," *IEEE Comun. Lett.*, vol. 19, no. 6, pp. 1069-1072, June, 2015.

[35] R. Koetter, A. C. Singer, and M. Tuchler "Turbo equalization," *IEEE Signal Process. Mag.*, vol. 21, no. 1, pp. 67-80, Feb. 2004.

[36] S. Sugiura, S. Chen, and L. Hanzo, "MIMO-aided near capcity turbo transcivers: Taxonomy and performance versus complexity," *IEEE Commun. Surveys Tuts.*, vol. 14, no. 2, pp. 421-442, May 2012.

[37] M. Tuchler, A. C. Singer, and R. Koetter, "Minimum mean squared error equalization: using a priori information," *IEEE Trans. Signal Process.*, vol. 50, no. 3, pp. 673-683, Mar. 2002.

[38] T. Abe and T. Matsumoto, "Space-Time turbo equalization in frequency-selective MIMO channels," *IEEE Trans. Veh. Technol.*, vol. 52, no. 3, pp. 469-475, May 2003.

[39] S. ten Brink, "Convergence behavior of iteratively decoded parallel concatenated codes,"*IEEE Trans. Commun.*, vol. 49, no. 10, pp. 1727-1737, Oct. 2001.

[40] M. E. Hajjar and L. Hanzo, "EXIT charts for system design and analysis," *IEEE Commun. Surveys Tuts.*, vol. 16, no. 1, pp. 127-153, Feb. 2014.

[41] E. Basar, U. Aygolu, E. Panayirci, and H. Vincent Poor, "Performance of spatial modulation in the presence of channel estimation errors," *IEEE Commun. Lett.*, vol. 16, no. 2, pp. 176-179, Feb. 2012.


**Lixia Xiao** received the B.E. and M.E. degrees in 2010 and 2013, respectively from University of Electronic Science and Technology of China (UESTC). Currently, she is working towards the Ph.D. degree in National Key Laboratory of Science and Technology on Communications in the same university. Her research is in the field of wireless communications and communication theory. In particular, she is very interested in signal detection and performance analysis of wireless communication systems.

**Yue Xiao** (M'04') received a Ph.D degree in communication and information systems from the University of Electronic Science and Technology of China in 2007. He is now an full professor at University of Electronic Science and Technology of China. He has published more than 30 international journals and been involved in several projects in Chinese Beyond 3G Communication R&D Program. His research interests are in the area of wireless and mobile communications.

This article has been accepted for publication in a future issue of this journal, but has not been fully edited. Content may change prior to final publication. Citation information: DOI 10.1109/TWC.2017.2713777, IEEE Transactions on Wireless Communications



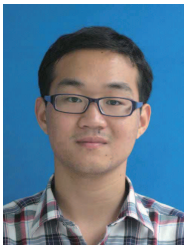

**Yan Zhao** received the B.E. degrees in commutation engineering from Zhengzhou University, Zhengzhou, China, in 2012. Since Sep. 2013, he is working towards the Ph.D. degree in National Key Laboratory of Science and Technology on Communications in University of Electronic Science and Technology of China (UESTC). Now his research interests include MIMO systems, non-orthogonal multiple access and communication signal processing.

**Ping Yang** (M'13'-SM'16') received the PhD degree in 2013 from University of Electronic Science and Technology of China (UESTC). From Sept. 2012 to Sept. 2013, he was a visiting student with the School of Electronics and Computer Science, University of Southampton, UK. From May 2014, he is a Research Fellow in EEE of NTU, Singapore. Also, he is an assistant professor at UESTC. His current research interests include MIMO/OFDM, machine learning, life science and communication signal processing.

**Marco Di Renzo** (S'05–AM'07–M'09–SM'14) was born in L'Aquila, Italy, in 1978. He received the Laurea (cum laude) and the Ph.D. degrees in Electrical and Information Engineering from the Department of Electrical and Information Engineering, University of L'Aquila, Italy, in April 2003 and in January 2007, respectively. In October 2013, he received the Habilitation à Diriger des Recherches (HDR) from the University of Paris–Sud XI, Paris, France.

Since January 2010, he has been a Tenured Academic Researcher ("Chargé de Recherche Titulaire") with the French National Center for Scientific Research (CNRS), as well as a faculty member of the Laboratory of Signals and Systems (L2S), a joint research laboratory of the CNRS, the École Supérieure d'Électricité (SUPÉLEC) and the University of Paris–Sud XI, Paris, France. His main research interests are in the area of wireless communications theory.

Dr. Di Renzo is the recipient of a special mention for the outstanding five-year (1997–2003) academic career, University of L'Aquila, Italy; the THALES Communications fellowship (2003–2006), University of L'Aquila, Italy; the 2004 Best Spin–Off Company Award, Abruzzo Region, Italy; the 2006 DEWS Travel Grant Award, University of L'Aquila, Italy; the 2008 Torres Quevedo Award, Ministry of Science and Innovation, Spain; the "Dérogation pour l'Encadrement de Thèse" (2010), University of Paris–Sud XI, France; the 2012 IEEE CAMAD Best Paper Award; the 2012 IEEE WIRELESS COMMUNICATIONS LETTERS Exemplary Reviewer Award; the 2013 IEEE VTC–Fall Best Student Paper Award; the 2013 Network of Excellence NEWCOM# Best Paper Award; the 2013 IEEE TRANSACTIONS ON VEHICULAR TECHNOLOGY Top Reviewer Award; the 2013 IEEE–COMSOC Best Young Researcher Award for Europe, Middle East and Africa (EMEA Region); and the 2014 IEEE ICNC Single Best Paper Award Nomination (Wireless Communications Symposium). Currently, he serves an an Editor of the IEEE COMMUNICATIONS LETTERS and of the IEEE TRANSACTIONS ON COMMUNICATIONS (Wireless Communications – Heterogeneous Networks Modeling and Analysis).

**Shaoqian Li** (F'16) received his B.S.E. degree in communication technology from Northwest Institute of Telecommunication (Xidian University) in 1982 and M.S.E. degree in Communication System from University of Electronic Science and Technology of China (UESTC) in 1984. He is a Professor, Ph.D supervisor, director of National Key Lab of Communication,UESTC, and member of National High Technology R&D Program (863 Program) Communications Group. His research includes wireless communication theory, anti-interference technology for wireless communications, spread-spectrum and frequency-hopping technology, mobile and personal communications.

**Wei Xiang** (S'00-M'04-SM'10) received the B. Eng. and M. Eng. degrees, both in electronic engineering, from the University of Electronic Science and Technology of China, Chengdu, China, in 1997 and 2000, respectively, and the Ph.D. degree in telecommunications engineering from the University of South Australia, Adelaide, Australia, in 2004. He is currently Foundation Professor and Head of Electronic Systems and Internet of Things Engineering in the College of Science and Engineering at James Cook University, Cairns, Australia. During 2004 and 2015, he was with the School of Mechanical and Electrical Engineering, University of Southern Queensland, Toowoomba, Australia. He is an IET Fellow, a Fellow of Engineers Australia, and an Editor for IEEE Communications Letters. He was a co-recipient of three Best Paper Awards at 2015 WCSP, 2011 IEEE WCNC, and 2009 ICWMC. He has been awarded several prestigious fellowship titles. He was named a Queensland International Fellow (2010-2011) by the Queensland Government of Australia, an Endeavour Research Fellow (2012-2013) by the Commonwealth Government of Australia, a Smart Futures Fellow (2012-2015) by the Queensland Government of Australia, and a JSPS Invitational Fellow jointly by the Australian Academy of Science and Japanese Society for Promotion of Science (2014-2015). In 2008, he was a visiting scholar at Nanyang Technological University, Singapore. During Oct. 2010 and Mar. 2011, he was a visiting scholar at the University of Mississippi, Oxford, MS, USA. During Aug. 2012 and Mar. 2013, He was an Endeavour visiting associate professor at the University of Hong Kong. He has published over 160 papers in peer-reviewed journal and conference papers. His research interests are in the broad area of communications and information theory, particularly coding and signal processing for multimedia communications systems.